

# Lightweight foam concrete containing expanded perlite and glass sand: Physico-mechanical, durability, and insulation properties



Osman Gencel<sup>a,\*</sup>, Oguzhan Yavuz Bayraktar<sup>b</sup>, Gokhan Kaplan<sup>c</sup>, Oguz Arslan<sup>d</sup>, Mehrab Nodehi<sup>e</sup>, Ahmet Benli<sup>f</sup>, Aliakbar Gholampour<sup>g</sup>, Togay Ozbakkaloglu<sup>e,\*</sup>

<sup>a</sup> Civil Engineering Department, Bartin University, 74100, Bartin, Turkey

<sup>b</sup> Civil Engineering Department, Kastamonu University, 37150, Kastamonu, Turkey

<sup>c</sup> Civil Engineering Department, Ataturk University, 25030, Erzurum, Turkey

<sup>d</sup> Department of Materials Science and Engineering, Kastamonu University, 37150, Kastamonu, Turkey

<sup>e</sup> Ingram School of Engineering, Texas State University, San Marcos, TX, USA

<sup>f</sup> Civil Engineering Department, Bingol University, 12100, Bingol, Turkey

<sup>g</sup> College of Science and Engineering, Flinders University, SA, Australia

## ARTICLE INFO

### Keywords:

Foam concrete  
Expanded perlite  
Waste glass  
Thermal insulation  
Thermal conductivity  
Durability properties  
Lightweight aggregate

## ABSTRACT

Foam concrete refers to a type of concrete with high porosity that can be produced with or without aggregate. Foam concrete has generally superior thermal insulation properties compared to conventional concrete. Despite its major thermal benefits, the high content of Portland cement, as well as its very high porosity, makes foam concrete prone to physico-durability concerns such as drying shrinkage by allowing the entrance of chemicals and free water to the concrete pores. To address this and reduce the pore network connectivity, in this study, expanded perlite and fine-sized waste glass sand were used as the main aggregates in concrete mixes. In that respect, 10 mixes of foam concrete were produced with two foam contents of 50 and 100 kg/m<sup>3</sup>, with a constant water-to-binder ratio (w/b) of 0.5. In each mix, the dominated expanded perlite aggregate was replaced by waste glass sand having a size of < 2.36 mm. Apparent porosity, water absorption, compressive and flexural strength, sorptivity, ultrasonic pulse velocity (UPV), drying shrinkage, freeze-thaw, alkali-silica reaction, thermal conductivity, and thermal resistance tests were performed to investigate the physico-mechanical, durability and insulation properties of the foam concrete. Based on the results, it is found that the addition of glass sand improves physico-mechanical and durability properties of foam concrete. The addition of expanded perlite increases the insulating properties of foam concrete, potentially due to the high porosity of expanded perlite compared to that of glass sand. The findings of this study point to the suitability of producing sustainable insulating foam concrete through the use of waste glass sand.

## 1. Introduction

The increasing trend in urbanization and industrialization that started since 19th century has caused a steadfast growth in energy consumption, material use and waste generation [1]. Although this trend is as a result of various human activities, construction industry is known to be a major contributor to the current environmentally unhealthy practices [2]. In that respect, it was reported that construction industry is responsible for up to 40% of the total energy consumption [3] and more than 8% of the total carbon dioxide (CO<sub>2</sub>) generation annually [4,5]. If unchanged, it is envisioned that this contribution can be up to 25% of the total CO<sub>2</sub> production by 2050 [6].

To reduce this trend and further optimize common practices, the use of sustainable high performance composite materials has been suggested and is being practiced. In construction industry, current trends in the production of insulating high performance materials can not only increase the energy efficiency of structures, but can also reduce the ecological footprint of the materials' processing and ultimate use [7]. Among commonly used materials, foam concrete is one of the outstanding materials that can have numerous applications in sustainable construction [8].

Foam concrete, also known as cellular concrete, is a type of lightweight concrete which is manufactured with a high porosity and void content and can be produced with or without using aggregates [9]. Since

\* Corresponding authors.

E-mail addresses: [ogencel@bartin.edu.tr](mailto:ogencel@bartin.edu.tr) (O. Gencel), [togay.oz@txstate.edu](mailto:togay.oz@txstate.edu) (T. Ozbakkaloglu).

its first introduction by Aylsworth and Dyer in 1914 [10,11] and then by Eriksson in the early 1920s [10,11], foam concrete has been most commonly known for its high thermal and acoustic insulation properties and adjustably low density. With a density range of commonly below 1600 kg/m<sup>3</sup>, foam concrete is highly workable with a variety of applications, such as a relatively cheap material for filling voids, ground stabilization, and most importantly, a major insulating material [12].

At the earlier stage of its development, however, foam concrete has been found to be unstable due to the segregation of air and solid phases [13], coalescence of adjacent bubbles [14] and the ripening effect (coarsening) of larger bubbles [15]. As a result, a variety of foaming techniques have been developed over time with the purpose of achieving homogeneously distributed air bubbles in the concrete. On this basis, chemical foaming [16], mechanical foaming [11,17], and foaming through heating and irradiation [18] have become the most commonly practiced methods of producing foam concrete. However, to produce a structural grade foam concrete, the use of proper aggregate is necessary. In this regard, the processing, transportation and effectively the use of a high quantity of aggregate can have major environmental implications such as depletion of natural resources [19]. In that respect, previous studies entertained the use of solid waste aggregates such as recycled concrete aggregates [20] and plastic waste [21] in the production of foam concrete, but they reported a significant rise in the porosity and water absorption and a reduction of thermal resistance of the produced foam concrete.

To utilize a porous, lightweight and compatible aggregate with foam structure, expanded perlite has been extensively used in the literature (e.g. [22,23]). In general, expanded perlite is a siliceous volcanic material that tends to expand in its size when subjected to temperatures of 900 to 1200 °C [16]. With a low density of around 240 kg/m<sup>3</sup> and a water absorption of generally ranging from 30 to 40%, expanded perlite has a lower density than expanded shale, slate and even pumice, and is a common lightweight material being used for different applications due to its chemical inertness and good thermal insulation [24,25]. In turn, among the most commonly available solid waste materials, glass is an amorphous and non-crystalline material with a high content of silicon [26–28] and has an estimated production rate of 100 million tons per annum [29]. Based on the study by Guo et al., [30], the top three types of produced glass include borosilicate, aluminosilicate, and soda-lime glass with slightly different chemical compositions. Although waste glass can be endlessly recycled to produce new glass [31], its recycling process requires high temperature for melting (at around 1600 °C) [31]. It was reported that such highly energy intensive process can produce 600 – 1500 kg of CO<sub>2</sub> for recycling of one ton of waste glass [32,33], and waste glass has a low recycling rate of around 26% [29]. Therefore, there is a great potential to use waste glass as a major supplement in concrete production. Although waste glass can be used as aggregate and powder in concrete, the grinding process of reducing the particle size of waste glass can have major energy and environmental implications [29,30]. As a result, in this study, fine-sized waste glass sand is used to replace the main aggregate, which is fine-sized expanded perlite.

The use of glass sand, however, has been reported to cause certain adverse effects on the concrete if not well-engineered. As was reported in the literature (e.g., [34–36]), the use of glass can result in increased likelihood of alkali-silica reaction (ASR) and increased content of free water in the pores that can cause freeze-thaw issues. According to Yang et al., [35], when the high content of reactive silica in glass particles is exposed to high alkalinity during the hydration, ASR gel is formed that later can exert internal expansive pressure and cause cracking. Park et al., [37] used glass aggregate with up to 70% substitution rate with sizes ranging 6 – 20 mm and reported a 44.3% reduction in the workability, 41.4% increased air content and up to 30% increased ASR expansion. Ismail and Al-hashmi [38] reported that the ASR tendency is directly related to the aggregate size and any size above 4.75 mm can develop ASR. Zhu et al., [34], Afshinna et al., [39], and Corinaldesi et al., [40] all recommended a different maximum size of glass aggregate

to avoid ASR. Du and Tan [41], however, reported that in more porous specimens, the expansion can be hosted in such pores.

To date, however, few studies have used glass sand in lightweight foam concrete production. Khan et al., [42] used crushed glass fine aggregate particles only as a filler in foam concrete and only conducted basic physico-mechanical tests (e.g., dry density and compressive strength tests). Schumacher et al., [43] used a combination of foam concrete with lightweight aggregates including expanded glass, and reported decreased drying shrinkage compared to the foam concrete with expanded perlite aggregate.

Based on the above-mentioned research gap in the literature, this study assessed physico-mechanical, durability, and insulation properties of foam concrete to ensure the propriety of the use of waste glass as a major aggregate material in the foam concrete. For this, 10 different mixes containing 0, 30, 50, 70, and 100% glass sand with two different contents of foam material (50 and 100 kg/m<sup>3</sup>) were produced. The results of this study are significant and point to the great potential of producing foam concrete with waste glass sand with excellent fresh, mechanical, durability and insulation properties. This can not only address natural resource conservation but can also produce a sustainable foam concrete with superior physico-mechanical and durability properties compared to normal foam concrete.

## 2. Experimental program

### 2.1. Materials

#### 2.1.1. Cement

In this study, general purpose cement CEM I 42.5 R (EN 197-1) with surface area of 3360 cm<sup>2</sup>/g was used as the binder material. The physico-chemical properties of the Portland cement is shown in Table 1.

#### 2.1.2. Aggregate

Expanded perlite and recycled glass sand (0–2.36 mm) with a specific gravity of 0.51 and 2.59 and water absorption of 143.2% and 0.32% were used as fine aggregate material, respectively. The glass sand was obtained from a local company specializing in the mounting of window glass. Waste glass released in the facility was transferred to the laboratory. In the laboratory, it was brought to sand size using a crusher. Figs. 1 and 2 show the x-ray powder diffraction (XRD) and thermogravimetric analysis (TGA) of the fine aggregates, respectively. Tables 2 and 3 present physical properties and sieve analysis results of the aggregates, respectively.

#### 2.1.3. Foam agent

The foaming agent used in this study had a density of 1.03 ± 0.02 kg/l, and contained enzyme-based proteins that can produce more homogeneous and stable bubbles, conforming to ASTM 869 [44]. The

**Table 1**  
Physico-chemical properties of Portland cement used in this study.

Physico-chemical properties	
SiO <sub>2</sub> (%)	13.66
Al <sub>2</sub> O <sub>3</sub> (%)	3.82
Fe <sub>2</sub> O <sub>3</sub> (%)	7.21
CaO (%)	67.53
MgO (%)	1.09
SO <sub>3</sub> (%)	4.05
Na <sub>2</sub> O <sub>(eqv)</sub> (%)	0.59
LOI (%)	1.21
Specific gravity	3.16
Specific surface area (cm <sup>2</sup> /g)	3360
Setting time (Initial/Final) (min)	175/220
Compressive strength (2 days) (MPa)	32.6
Compressive strength (28 days) (MPa)	52.3
Le Chatelier (mm)	0.9

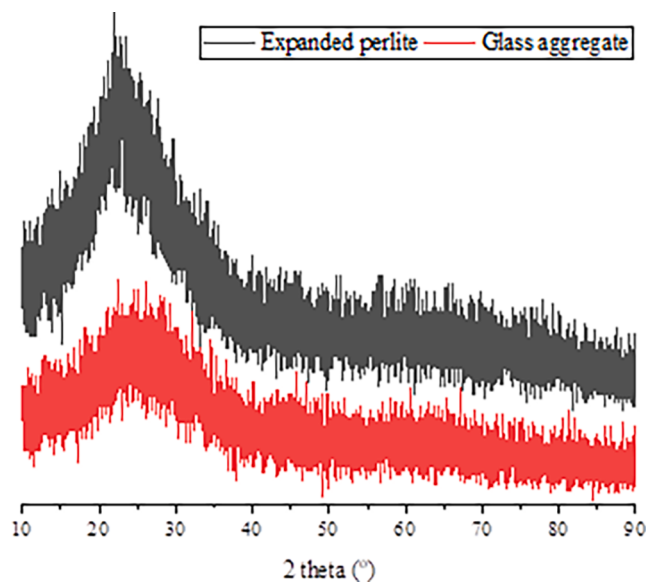


**Fig. 1.** XRD of expanded perlite and glass sand.

foaming agent was secured from a local industry with commercial name of Aydos Construction Chemicals-TURKEY. The other properties of the foaming agent are presented in Table 4.

## 2.2. Mix proportions

In this study, 10 foam mixes were prepared in total with a constant water-to-binder ratio (w/b) of 0.5. In the mixes, expanded perlite was replaced with 0, 30, 50, 70, and 100 vol% of the glass sand. Foaming agent was used in two volumetric quantities of 50 and 100 kg/m<sup>3</sup>. To induce internal curing, the expanded perlite aggregates were pre-soaked in water in an ambient temperature. Mixes in this study have been designed based on the authors' previous experiments with foam concrete (e.g., [45]). The mixing was done through mixing dry materials initially for 60 s. Water was then added and the mixing continued for another 120 s. Finally, the foaming agent was added and the mixing continued for another 60 s.

Table 5 shows the mix proportions used in this study. In Table 5 the mixes are labelled as follows: letters G and F refer to glass sand and foam agent, respectively. The following numbers after each letter indicate the content of each material in the mix (% for glass sand and kg/m<sup>3</sup> for foam agent). For example, G50F100 represents a foam mix containing 50% glass sand and 100 kg/m<sup>3</sup> foam agent.

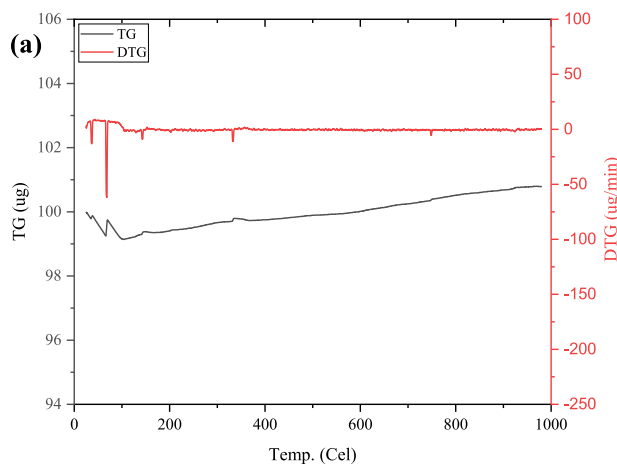


**Table 2**

Physical properties of expanded perlite and glass sand used in this study.

Information	Expanded perlite	Glass sand
Specific gravity	0.51	2.59
Water absorption (%) 24 h (by mass)	143.2	0.32
Color	White	White

**Table 3**

Sieve analysis of expanded perlite and glass sand used in this study based on ASTM C 136 [104].

Sieve size (mm)	Passing (%)	
	Expanded perlite	Glass sand
4.75	99.8	99.9
2.36	99.6	99.7
1.18	82.2	78.5
0.600	41.2	43.8
0.300	16.4	18.4
0.150	2.4	1.9
< 0.150	—	—

**Table 4**

Properties of the foaming agent used in this study.

Chemical contents	Synthetic liquid air-entraining	
Appearance (color)	Translucent, pale brown liquid	
Density	1.03 ± 0.02	ISO 758 kg/l.
pH value	5.0 ± 1	TS 6365 EN 1262
Chloride content (Cl)	< % 0.1	TS EN 480-10
Alkali content	< % 5	TS EN 480-12
Freezing point	– 5 °C	



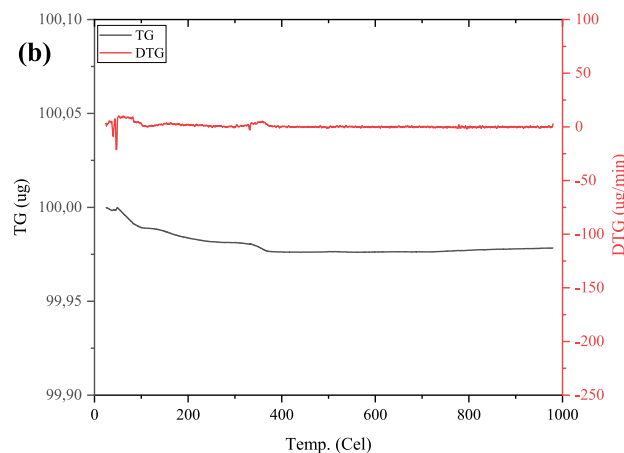


**Fig. 2.** TGA curves of (a) glass sand and (b) expanded perlite.

**Table 5**

Mix proportions used in this study.

Mix ID	Glass sand (%)	Expanded perlite (%)	Cement (kg/m <sup>3</sup> )	Expanded perlite (kg/m <sup>3</sup> )	Glass sand (kg/m <sup>3</sup> )	Water (kg/m <sup>3</sup> )	Foam (kg/m <sup>3</sup> )	Pre-soaked water for perlite (kg/m <sup>3</sup> )
G0F50	0	100	350	231	0	175	50	231.0
G30F50	30	70		161.7	360.4			161.7
G50F50	50	50		115.5	600.7			115.5
G70F50	70	30		69.3	841.0			69.3
G100F50	100	0		0	1201.5			0
G0F100	0	100		106.0	0		100	106.0
G30F100	30	70		74.2	165.4			74.2
G50F100	50	50		53.0	275.7			53.0
G70F100	70	30		31.8	386.0			31.8
G100F100	100	0		0	551.5			0

### 2.3. Specimen preparation and test methods

**Table 6** presents details on the testing methods conducted in this study, including specimens' size, relevant ASTM standards, and testing condition. To assess the workability of the mixes, flow table test conforming to ASTM C230 [46] was performed. Physical properties of the foamed concrete, including bulk density, porosity, water absorption and sorptivity were measured using 50 × 50 × 50 mm specimens after 28 days of curing based on ASTM C29 [47], ASTM C20 [48], ASTM C948 [49] and ASTM C1585 [50], respectively.

For mechanical properties, after casting the specimens and demolding them in 24 h, the specimens were cured in water conditions at 20 °C until testing day. In that regard, six and three specimens were made for each compressive and flexural strengths test, and their mean value has been calculated and reported. The compressive and flexural strengths tests were complied to ASTM C 349 [51] and ASTM C 348 [52], respectively, and were measured at 7, 28, 91, and 120 days of curing.

To measure durability of the mixes, drying shrinkage, freeze–thaw, and ASR tests were conducted conforming to ASTM C 596 [53], ASTM C 666 [54], and ASTM C 1260 [55], respectively. Drying shrinkage test was performed till 120 days of curing. For the ASR test, the specimens were immersed in 80 °C NaOH initially for 14 days and then they were kept at 23 °C NaOH until the 120th day. As for the freeze–thaw resistance test, 25 freeze–thaw cycles were used on 40 × 40 × 160 mm specimens conforming to ASTM C666 [54].

**Table 6**  
Experiments conducted in this study along with other details.

Experiment	Standard	Specimen size (mm)	Time
Flow diameter	ASTM C 230 [46]	–	Fresh mortar
Apparent porosity and water absorption	ASTM C20 [48]	50 × 50 × 50	28 days
Bulk density (Hardened) (with caliper)	–	50 × 50 × 50	28 days
Compressive strength	ASTM C 349 [51]	40 × 40 × 160	7, 28, 91 and 120 days
Flexural strength	ASTM C 348 [52]		
Sorptivity	EN 1015-18	50 × 50 × 50	28 days
Drying shrinkage	ASTM C 596 [53]	25 × 25 × 285	120 days
Freezing and thawing	ASTM C 666 [54]	40 × 40 × 160	25 cycles
Alkali-silica reaction*	ASTM C 1260 [55]	25 × 25 × 285	120 days
High temperature** (Slow cooling-air) (Rapid cooling-water)	–	40 × 40 × 160	200, 400, 600 and 800 °C
Thermal conductivity	–	50 × 100 × 20	28 days

\*80 °C NaOH for 14 days then 23 °C NaOH until the 120th day.

\*\*Heating rate: 10 °C /min.

Finally, to assess the thermal performance of the specimens, thermal conductivity test was performed on the specimens with the size of 50 × 100 × 20 mm after 28 days of curing and the high temperature resistance test was performed on 40 × 40 × 160 mm specimens. To evaluate the thermal resistance of the specimens, four temperature levels of 200, 400, 600, and 800 °C with the heating rate of 10 °C/min were adopted under two different cooling conditions of slow cooling in air and rapid cooling by immersion of the specimens in water right after being heated. In conjunction with the thermal resistance test, ultrasonic pulse velocity (UPV) test was also conducted to further evaluate the physico-mechanical properties of the mixes right after being subjected to the thermal stress.

Scanning electron microscopy (SEM) and energy dispersive spectroscopy (EDS) were performed on G0F100, G50F50 and G100F100 mixes after 25 cycles of ASR and exposed to high temperature of 800 °C to analyze the microstructure and chemical composition of foam concretes.

### 3. Test results and discussions

#### 3.1. Flowability

The result of the flow table test on different specimens is shown in Fig. 3. Based on the figure, the overall flow diameter was recorded to range from 138 mm for the mix having 100 kg/m<sup>3</sup> of foam with 100% expanded perlite aggregate to 219 mm for the mix having 50 kg/m<sup>3</sup> of foam with 100% glass sand. It can be seen in the figure that, for a given foam content, the addition of glass sand increased the flowability of the mix. In addition, an increase in the glass sand content led to an increase in the flowability of the mixes at a given foam agent content. Mixes with 50 kg/m<sup>3</sup> and 100 kg/m<sup>3</sup> foam agent containing 100% glass sand exhibited ~ 55% higher flowability compared to the companion mixes containing 100% expanded perlite. The higher flowability of the mixes containing a higher glass sand content can be related to the smooth surface of glass particles that enhance the flowability of the mix [29]. This observation is aligned with that of previous studies [56–59].

It can also be seen in Fig. 3 that, for a given glass sand content, an

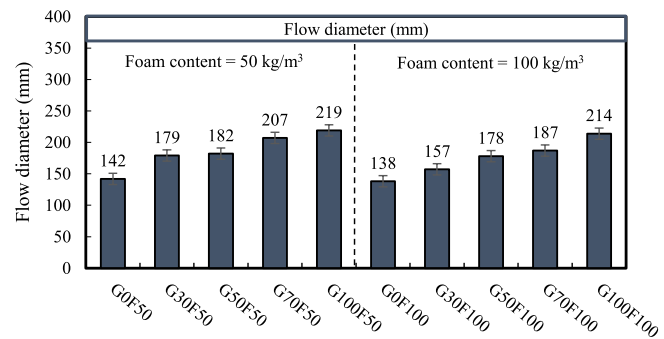


Fig. 3. Flow table test results of different mixes.

increase in the foam agent content from  $50 \text{ kg/m}^3$  to  $100 \text{ kg/m}^3$  caused  $\sim 6\%$  decrease in the flowability of the mix. This observation can be due to the increased stable air bubbles with an increased foam content in the mix, or as Refs. [60,61] noted, it can be due to the increased adhesion between stable air bubbles and solid particles since each bubble tends to hold some water content in itself that results in increased stiffness with an increased foam agent content.

### 3.2. Compressive strength

According to previous studies [11,16], the most influential parameters on the compressive strength of foam concrete are the overall porosity, presence of aggregate and fillers, w/b ratio and curing regime. Fig. 4(a) shows the mean compressive strength of different mixes at 7, 28, 91 and 120 days of curing. Based on the figure, the highest and lowest compressive strengths achieved were for G100F50 (5.32 MPa at 120 days of curing) and G0F100 (1.19 MPa at 120 days of curing), respectively. It can be seen in the figure that an increase in the foam content from  $50 \text{ kg/m}^3$  to  $100 \text{ kg/m}^3$  reduced the compressive strength of the mixes by  $\sim 62, 64, 74$ , and  $72\%$  at 7, 28, 91 and 120 days of curing, respectively. This observation is consistent with previous studies on the effect of foaming agents on mechanical properties and can be attributed to the increased porosity of the mixes with an increased foam content [62,63].

As can also be seen in Fig. 4(a), the addition of glass sand steadily increased the compressive strength of the mix for a given foam content and curing age. At  $50 \text{ kg/m}^3$  foam content, mixes containing 30, 50, 70, and 100% glass sand had  $\sim 20, 21, 31$ , and  $33\%$  higher compressive strength than that containing 0% glass sand, respectively. At  $100 \text{ kg/m}^3$  foam content, mixes containing 30, 50, 70, and 100% glass sand had  $\sim 2, 5, 8$ , and  $14\%$  higher compressive strength compared to that containing 0% glass sand, respectively. These results indicate that the addition of glass sand has a more positive effect on the strength development of the mixes with a lower content of foam agent, which can be due to the better surface adhesion of the glass sand with paste matrix in a less porous mix [64]. According to Ref. [60], a lower content of foam leads to a higher solid content within the mix, which results in a larger content of available solid materials to bind with the aggregates' surface, resulting in an enhanced compressive strength. The lower strength of mixes with a higher perlite aggregate content is aligned with previous studies that reported the mix containing perlite aggregates have a comparatively lower strength compared to those containing river sand and glass sand [16,23,65]. The reason for this behavior can be the higher porosity of mixes containing higher perlite aggregates than those containing higher glass sand, as it is shown in section 3.5, which resulted in a lower overall strength of the mixes containing a higher perlite aggregate.

### 3.3. Flexural strength

Fig. 4(b) shows the results of the flexural strength of different specimens at 7, 28, 91 and 120 days of curing. As can be seen in the figure, unlike for the compressive strength, specimens reached most of their flexural strength at 28 days of curing. In addition, the effect of a higher content of foam on the flexural strength is less pronounced compared to that on the compressive strength. Based on Fig. 4(b), the highest and lowest flexural strengths achieved were for G100F50 (1.47 MPa at 120 days of curing) and G0F100 (0.24 MPa at 7 days of curing), respectively. It can be seen in the figure that, for 0% glass content, an increase in the foam content from  $50 \text{ kg/m}^3$  to  $100 \text{ kg/m}^3$  reduced the flexural strength of the mixes by  $\sim 40, 56, 58$ , and  $56\%$  at 7, 28, 91 and 120 days of curing, respectively. On average, mixes with  $50 \text{ kg/m}^3$  foam content had about 55% higher flexural strength than their companion mixes with  $100 \text{ kg/m}^3$  foam. The observation on the higher flexural strength of the mixes with a lower foam content is aligned with that of previous studies [66–68], and can be due to the higher content of solid materials in the

mixes with a lower foam content to withstand internal stresses.

Additionally, at  $50 \text{ kg/m}^3$  foam content, mixes containing 30, 50, 70, and 100% glass sand had  $\sim 11, 5, 5.9$ , and  $5\%$  higher flexural strength than those containing 0% glass sand, respectively. At  $100 \text{ kg/m}^3$  foam content, mixes containing 30, 50, 70, and 100% glass sand had  $\sim 8.2, 4.4, 7.2$ , and  $5.4\%$  higher flexural strength compared to that containing 0% glass sand, respectively. As mentioned earlier in section 3.3, the higher strength of mixes containing a higher glass sand can be attributed to the lower porosity of mixes containing higher glass sand than those containing higher perlite aggregate.

Fig. 4(c) shows the compressive-to-flexural strength ratio of different mixes at 7, 28, 91 and 120 days of curing. According to the figure, an increase in the curing time generally led to a decrease in the compressive-to-flexural strength ratio of foam concretes, indicating a higher flexural strength development compared to the compressive strength development in foam concretes at later ages. As can also be seen, an increased foam content caused a decrease in the compressive-to-flexural strength ratio of foam concretes for a given curing age and aggregate content, indicating that the foam content has a higher impact on the compressive strength than that of the flexural strength. It is also shown in Fig. 4(c) that the mixes having a higher content of glass sand had generally a lower compressive-to-flexural strength ratio. This observation indicates that the higher content of glass sand is more effective in increasing the flexural strength than that of the compressive strength of foam concrete.

### 3.4. Bulk density

Variation in density value can play a direct role in mechanical and thermal insulation properties of foam concrete [17,69]. Fig. 5 shows the dry bulk density of different mixes at 28 days of curing. As can be observed in the figure, the dry bulk density of foam concretes of this study ranged from  $594 \text{ kg/m}^3$  for G0F100 mix to  $1504 \text{ kg/m}^3$  for G100F50 mix. Based on the figure, for a given glass sand content, an increase in the foam agent content from  $50 \text{ kg/m}^3$  to  $100 \text{ kg/m}^3$  caused  $\sim 31\%$  reduction in the dry bulk density of foam concrete.

As can be seen in Fig. 5, for a given foam content, the addition of glass sand increased the bulk density of the mix, with a more significant increase for the mixes containing  $50 \text{ kg/m}^3$  foam than those containing  $100 \text{ kg/m}^3$  foam. At  $50$  and  $100 \text{ kg/m}^3$  foam content, the mix containing 100% glass sand had 69% and 81% higher bulk density than the companion mix containing 0% glass sand, respectively. The increase in the bulk density with an increased glass sand content can be due to the higher specific gravity of glass sand compared to that of the expanded perlite, as was shown in Table 2.

### 3.5. Porosity and water absorption

Fig. 6 shows the water absorption and apparent porosity test results on different mixes at 28 days of curing. According to the figure, the highest water absorption and apparent porosity achieved were for G0F100 (54.52% and 74.54%, respectively) and the lowest were for G100F50 (15.30% and 21.65%, respectively). It can also be seen that, for a given glass sand content, an increased foam content from  $50 \text{ kg/m}^3$  to  $100 \text{ kg/m}^3$  increased the water absorption (21–117%) and apparent porosity (23–162%) of the foam concrete. The higher water absorption of the mixes containing a higher foam content can be because of the more porous microstructure of the mixes containing a higher foam content than those containing a lower foam content.

As can also be observed in Fig. 6, for a given foam content, the addition of glass sand steadily decreased the water absorption and porosity of foam concrete. This observation can be attributed to the filler effect of fine-sized glass sand, which decreases the porosity of the microstructure of the foam concrete. As was shown in Table 2, glass sand had a lower water absorption than expanded perlite, which resulted in a decreased water absorption of the foam concrete with an increased glass

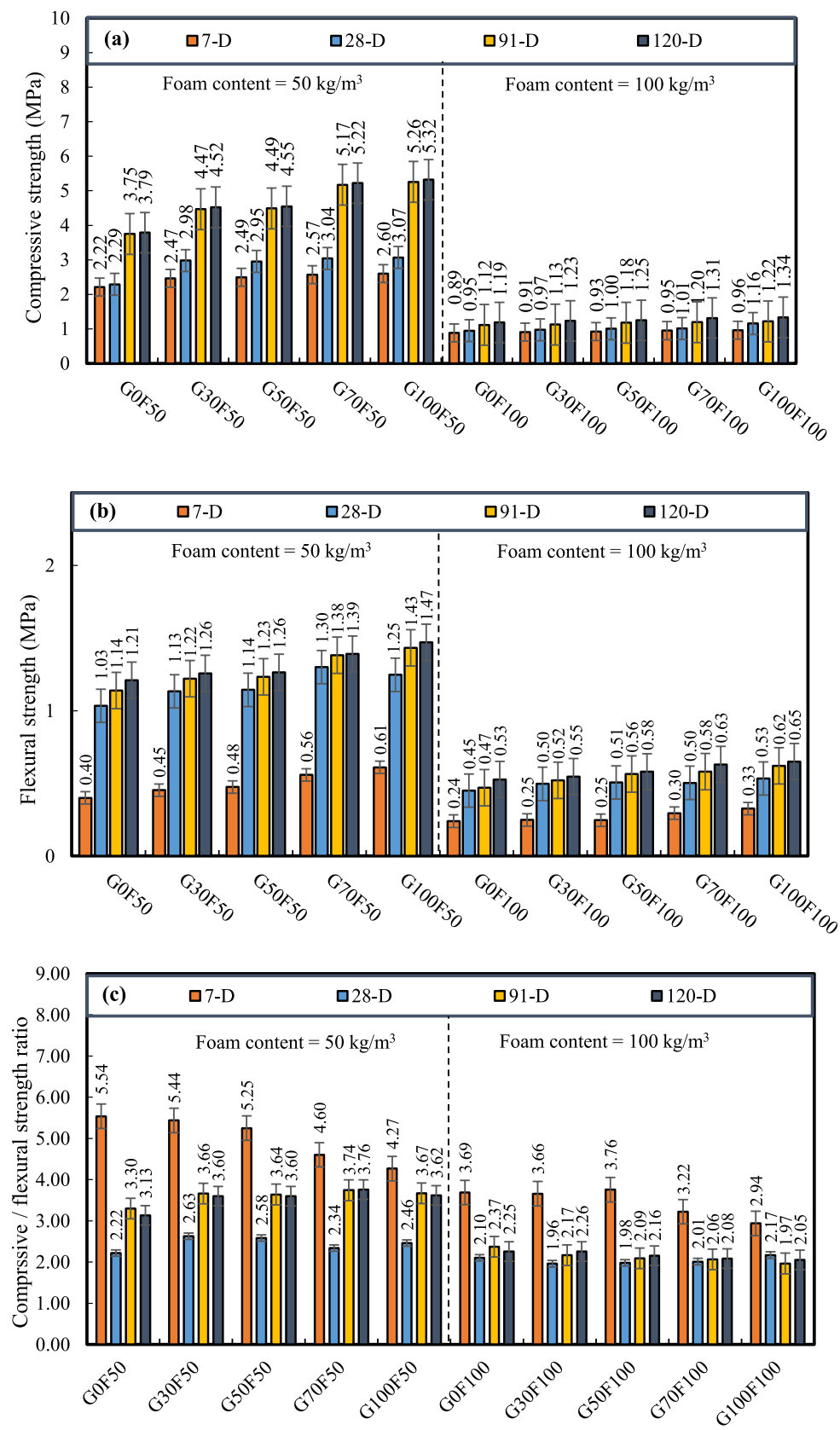


Fig. 4. Mean values of (a) compressive strength, (b) flexural strength, and (c) compressive-to-flexural strength of different mixes.

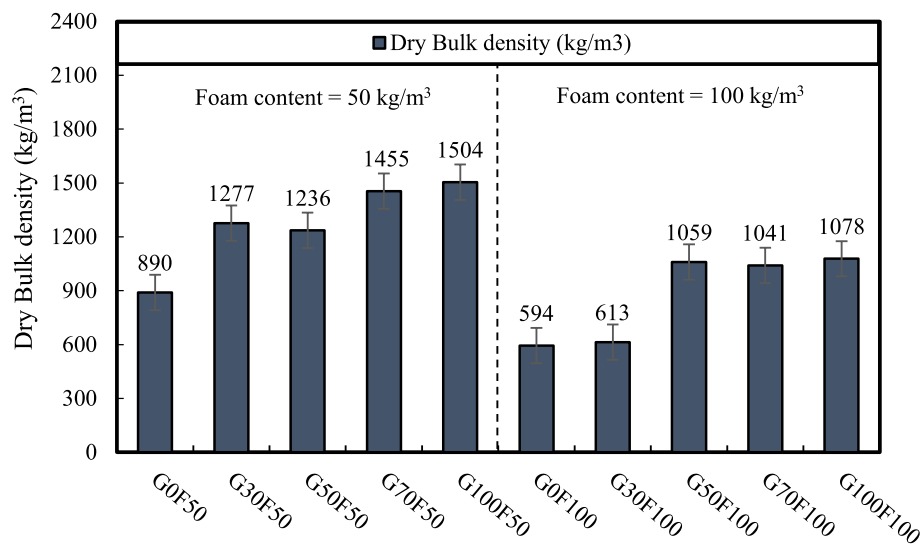


Fig. 5. Dry bulk density of different mixes at 28 days of curing.

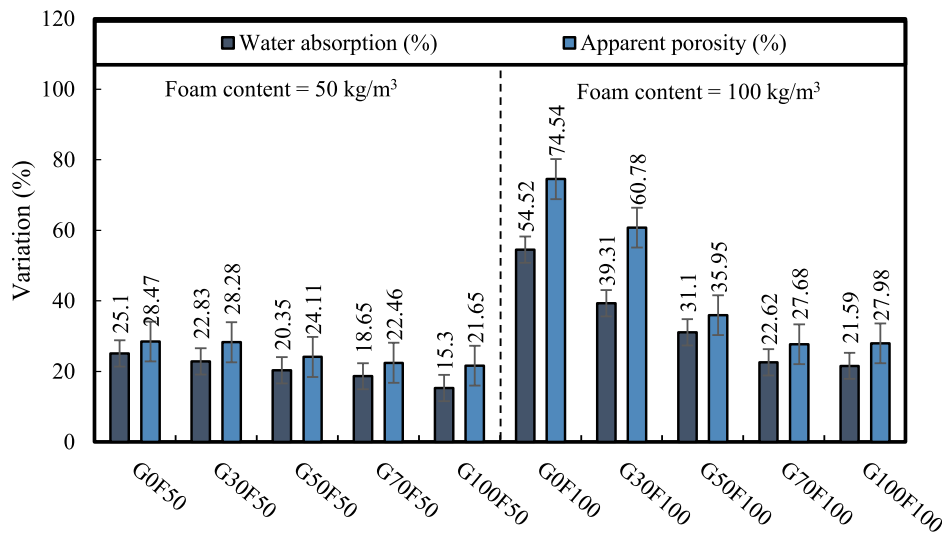


Fig. 6. Water absorption and apparent porosity of different mixes at 28 days of curing.

sand content. These results are aligned with previous studies, which showed that glass sand can fill the pores and reduce water absorption [70,71]. At 50 kg/m<sup>3</sup> foam content, the mix containing 100% glass sand had 39% and 24% lower water absorption and apparent porosity, and at 100 kg/m<sup>3</sup> foam content, the mix containing 100% glass sand had 60% and 62% lower water absorption and apparent porosity compared to the companion mixes containing 0% glass sand, respectively. The less significant influence of the addition of glass sand on decreasing the porosity of foam concrete containing 50 kg/m<sup>3</sup> can be attributed to the lower pore network connectivity of the 50 kg/m<sup>3</sup> foam concrete when the matrix has a higher solid content [60].

### 3.6. Sorptivity

Sorptivity refers to the rate of penetration of liquid materials that is also related to the effective porosity of the concrete mix [72]. Fig. 7 shows the result of sorptivity test on different mixes conducted after 28 days of curing. According to the figure, at 0% glass sand, the mix containing 100 kg/m<sup>3</sup> foam content (G0F100) exhibited three times higher sorptivity rate than the mix containing 50 kg/m<sup>3</sup> foam content (G0F50). This observation can be attributed to the lower solid content and higher

capillary porosity of the matrix of G0F100 compared to those of G0F50, leading to higher pore network connectivity in G0F100 as was reported by Refs. [70,71].

Yet, for a given foam content, as the content of glass sand increased, the sorptivity rate decreased significantly. This can be due to both impermeability of glass sand, as well as their effectiveness in filling larger pores and reducing the pore network connectivity, as noted by Refs. [60,64]. Also, based on Fig. 7, it can be seen that as the curing period increases the sorptivity rate in some mixes containing higher glass sand content appeared to decrease. As was reported by Refs. [29,73], glass particles have some surface reactivity that generally takes longer to react. Such adhesion can explain the reason behind slight lowering tendency of sorptivity rate experienced in this study.

### 3.7. Drying shrinkage

Drying shrinkage refers to the concrete moisture loses, most commonly due to the interaction with the surrounding environment, causing an internal shrinking stress that can result in cracking and a loss of physico-mechanical properties of concrete [29]. It was reported that the use of porous and anhydrite materials in the concrete mix as well as

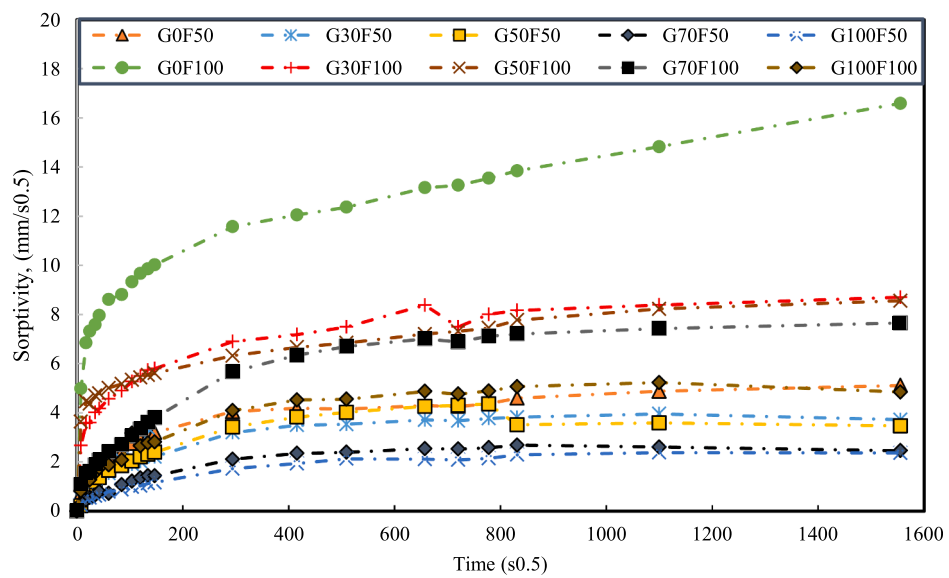
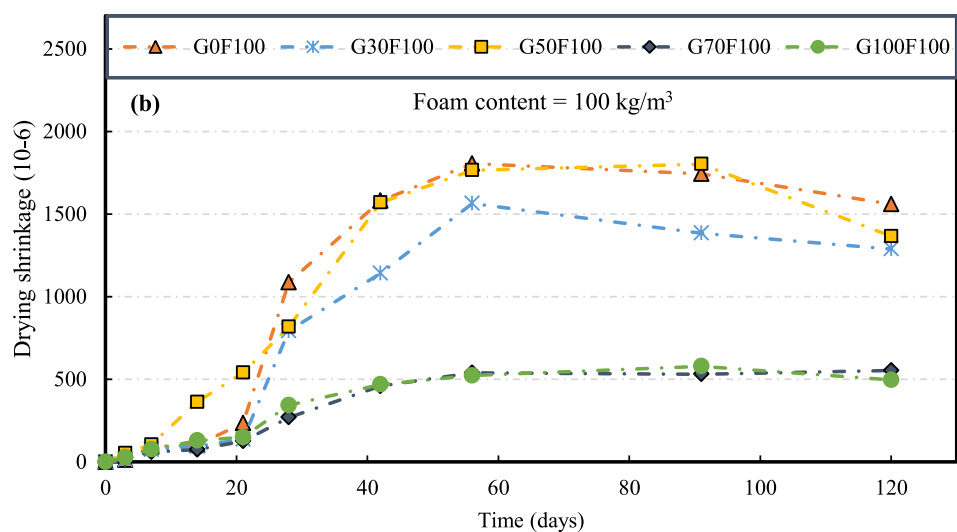
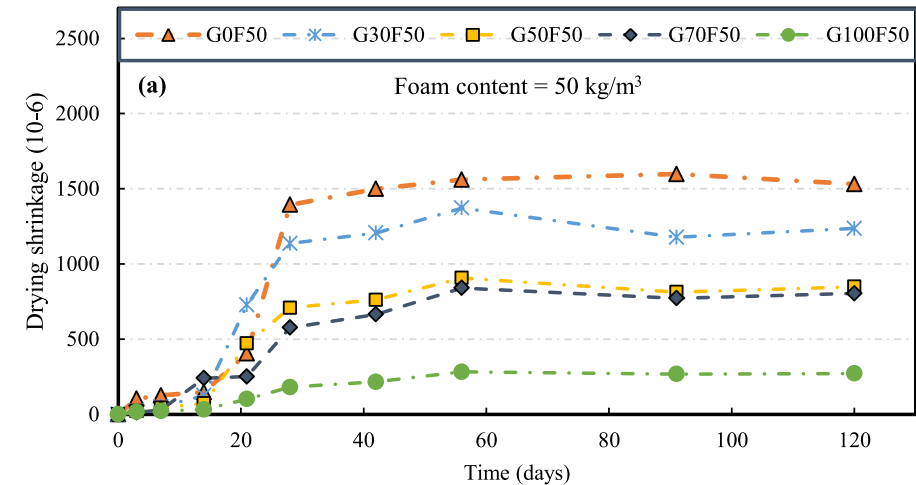


Fig. 7. Sorptivity rate of different mixes.

Fig. 8. Drying shrinkage of different mixes containing (a) 50 kg/m<sup>3</sup> and (b) 100 kg/m<sup>3</sup> foam agent.

thermal curing potentially reduces the moisture content of concrete, resulting in an increased drying shrinkage [29]. Yet, since the overall porosity and pore size of foam concrete can potentially be higher than those of normal concrete, previous studies (e.g., [11,74]) reported that foam concrete can experience about 5 to 10 times higher drying shrinkage compared to the normal concrete. Such high drying shrinkages in foam concrete were reported to be due to the comparatively lower content of aggregate in the foam concrete to resist the internal stresses as a result of shrinkage compared to that of the normal concrete [11,74].

Fig. 8 shows the drying shrinkage of different mixes during their 120 days of curing. As can be observed in the figure, at 120th day, the drying shrinkage of foam concretes of this study ranged from 271  $\mu\epsilon$  ( $10^{-6}$ ) for G100F50 to 1560  $\mu\epsilon$  ( $10^{-6}$ ) for G0F100. Based on the figure, for 0% glass content, an increase in the foam agent content from 50 kg/m<sup>3</sup> to 100 kg/m<sup>3</sup> caused ~ 2% increase in the drying shrinkage of foam concrete. The same trend of having a higher shrinkage can be observed for mixes with a higher foam content. In the same way, as can be seen in Fig. 8, at 50 and 100 kg/m<sup>3</sup> foam content, the mix containing 100% glass sand had ~ 82% and 68% lower drying shrinkage than the companion mix containing 0% glass sand, respectively. The lower drying shrinkage of mixes containing a higher glass content agrees with previous studies

on the effect of glass particles in reducing the drying shrinkage (e.g., [75,76]), and can be due to the lower water absorption as a result of impermeability of glass particles [59] and more smooth surface of glass sand, which can potentially allow moisture to be transported [29], than those of expanded perlite aggregates, enhancing water dispersion in the mix that reduces the drying shrinkage [29,76].

### 3.8. Alkali-silica reaction (ASR)

In general, ASR refers to a chemical reaction that takes place between the cement paste and the alkaline ( $\text{Na}^+$  and  $\text{K}^+$ ) and hydroxyl ( $\text{OH}^-$ ) ions [29,77]. Although ASR is specifically not a major issue in foam concrete, the use of glass sand is often associated with relatively increased ASR, potentially due to the sodium content (Na) of glass material [29]. Previous studies (e.g., [34,40,78]) reported that the degree of expansion is in close relationship with the glass particle sizes. Most commonly, it was reported that a glass size of below 4.75 does not increase ASR [29,38]. In this study, the glass sand used had a particle size of < 2.36 mm.

Fig. 9 shows the ASR expansion of different specimens at different curing ages. As can be observed in the figure, at 120th day of curing, the ASR of foam concretes of this study ranged from 0.093% for G50F50 to

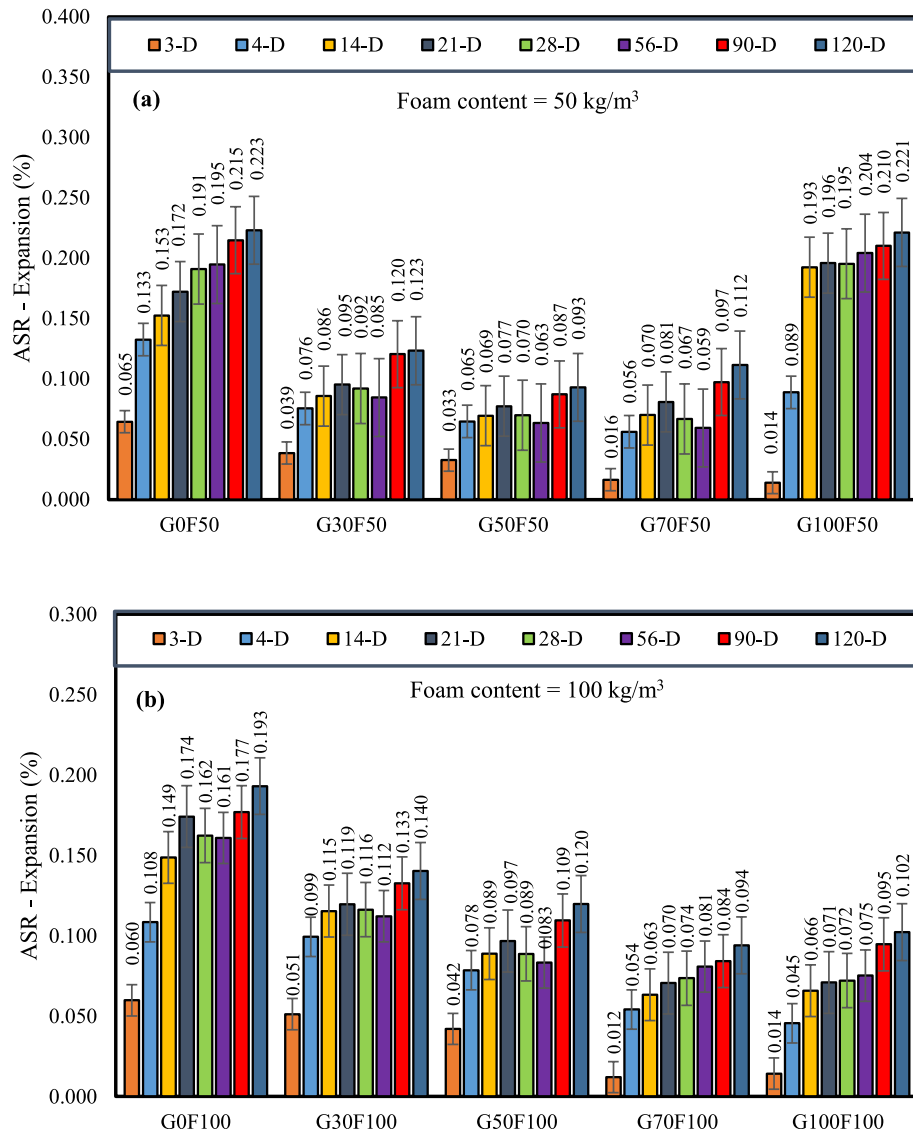


Fig. 9. The result of ASR test on different mixes containing (a) 50 kg/m<sup>3</sup> and (b) 100 kg/m<sup>3</sup> foam agent.

0.223% for G0F50. It is shown in the figure that, for a given glass sand content, mixes with a higher foam content exhibited generally a lower ASR expansion. This observation is due to the more porous microstructure of the mix with a higher foam content, leading to the accommodation of the expansion of more ASR gels inside the pores compared to those with a less foam content [79].

As can also be observed in Fig. 9, at 50 kg/m<sup>3</sup> and 100 kg/m<sup>3</sup> foam content, mixes containing glass sand had generally a less ASR expansion than the companion mixes without glass sand. In addition, an increase in the glass sand content led to a decrease in the ASR expansion of foam concretes, except for the G100F50 mix, which exhibited generally a higher ASR expansion than G70F50 mix. The ASR expansion reduction with an increased glass sand content is aligned with the SEM and EDS analysis results presented in Sections 3.12.1 and 3.12.2, and the results of previous studies that reported a reduction of ASR expansion when glass sands with the size of < 4.75 mm were used [38,39,80].

According to Refs. [81–84], a reduction of ASR is commonly known to be due to dilution of alkalis, accommodation of ASR gel by the porosity of the paste, a reduction in permeability of the concrete that reduces the mobility of ions, or the effect of high silica content that reacts and can host alkalis in its paste matrix. The results achieved in this study (the decrease of the ASR expansion with an increased glass sand content) point to the potential effect of lower permeability and surface reactivity of glass particles.

Based on Fig. 9, at 120 days of curing, 50 and 100 kg/m<sup>3</sup> foam mixes containing 30, 50, 70 and 100% glass sand experienced ~ 38% and 32% less ASR expansion than those companion mixes without glass sand, respectively. As can also be seen from Fig. 9, the 3-day ASR expansion of mixes having glass sand was considerably low. On average, 50 and 100 kg/m<sup>3</sup> foam mixes containing 30, 50, 70 and 100% glass sand experienced ~ 60% and 50% lower early expansion (at 3 days) compared to the companion mixes without glass sand, respectively. These observations are aligned with previous studies that reported the addition of fine glass sand can reduce ASR expansion through enhanced dispersion of alkalis [29].

### 3.9. Freeze-thaw resistance

Freeze-thaw resistance refers to the ability of the concrete to withstand the internal stresses caused by the formation of ice at low temperatures in concrete's pores [85]. The formation of ice can enlarge the size of pores and increase their respective tortuosity [85]. In foam concrete, the freeze-thaw effect can be more significant than that in the normal concrete since the overall porosity of foam concrete is relatively higher and more water-filled pores will be available compared to normal concrete [85].

Fig. 10(a) and (b) show the effect of 25 cycles on the compressive and flexural strengths of different mixes, respectively. Based on the figures, exposing the mixes to freeze-thaw cycles led to a decrease in the strength of foam concrete. At 50 and 100 kg/m<sup>3</sup> foam content, mixes after freeze-thaw experienced ~ 13.2% and 36.2% lower compressive strength and 6.9% and 12.7% lower flexural strength than mixes before freeze-thaw, respectively. This observation is aligned with the results of the previous study on fly ash-based foam concrete with 50 kg/m<sup>3</sup> foam content and under 25 cycles of freeze-thaw, which showed that the compressive strength of the foam concrete decreased by 15% after freeze-thaw cycles [86].

Fig. 10(c) shows the mass loss of different mixes after 25 freeze-thaw cycles. Based on the figure, the mass loss values ranged from 12.19% for G0F100 to 5.40% for G100F100. It can be seen from the figure that the mixes with a higher foam content experienced generally a higher mass loss (14–60%) than those with a lower foam content. The mass loss increase with an increased foam content is owing to the decreased content of solid materials in the mix to withstand the internal stresses caused by freeze-thaw [85]. This observation is aligned with previously reported studies on fly ash-based foam concrete [85,87]. It can also be seen that,

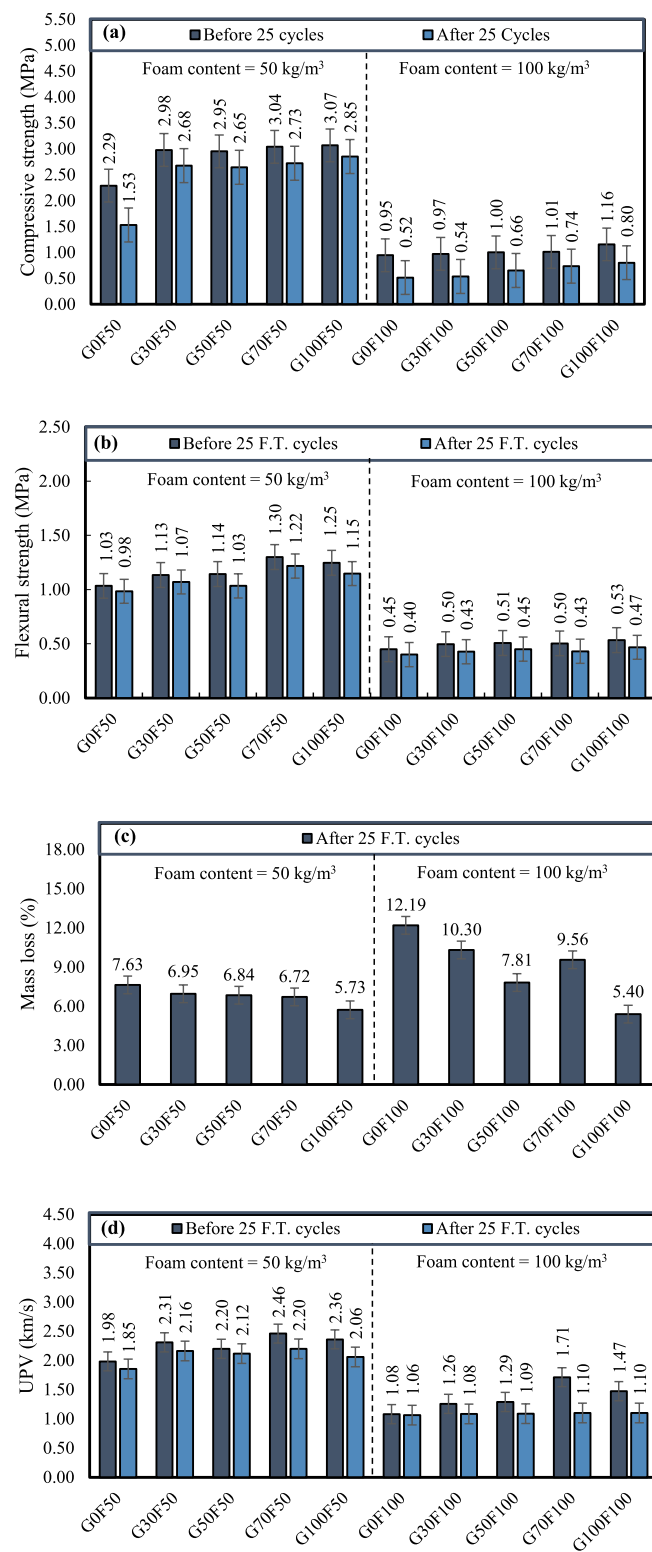


Fig. 10. The effect of freeze-thaw (25 cycles) on (a) compressive strength, (b) flexural strength, (c) mass loss, and (d) UPV of different mixes.

for a given foam content, an increase in the glass sand content generally led to a decrease in the mass loss of foam concretes. The higher mass loss of the mixes at a lower glass sand content can be due to the lower strength of expanded perlite compared to that of glass sand to withstand the internal stress caused by freeze-thaw cycles [88].

Fig. 10(d) shows the results of UPV conducted on different mixes

before and after freeze-thaw cycles. According to the figure, for a given foam and glass sand content, exposing the mixes to freeze-thaw cycles led to a decrease in the UPV speed of foam concrete. This observation is due to the formation of higher voids and internal cracks as a result of freeze-thaw cycles [89]. Based on Fig. 10(d), the UPV speed of foam concrete after freeze-thaw ranged from 1.06 km/s for G0F100 to 2.20 km/s for G70F50. It can also be observed in the figure that, for a given glass sand content, an increase in the foam agent content from 50 kg/m<sup>3</sup> to 100 kg/m<sup>3</sup> caused ~ 47% decrease in UPV speed of foam concrete after 25 freeze-thaw cycles. This observation agrees with previous studies [9,90]. In general, the freeze thawing performance of glass sand mixes is found to be superior than expanded perlite potentially due to lowered permeability in the skeleton of glass sand [88,90].

### 3.10. Thermal conductivity

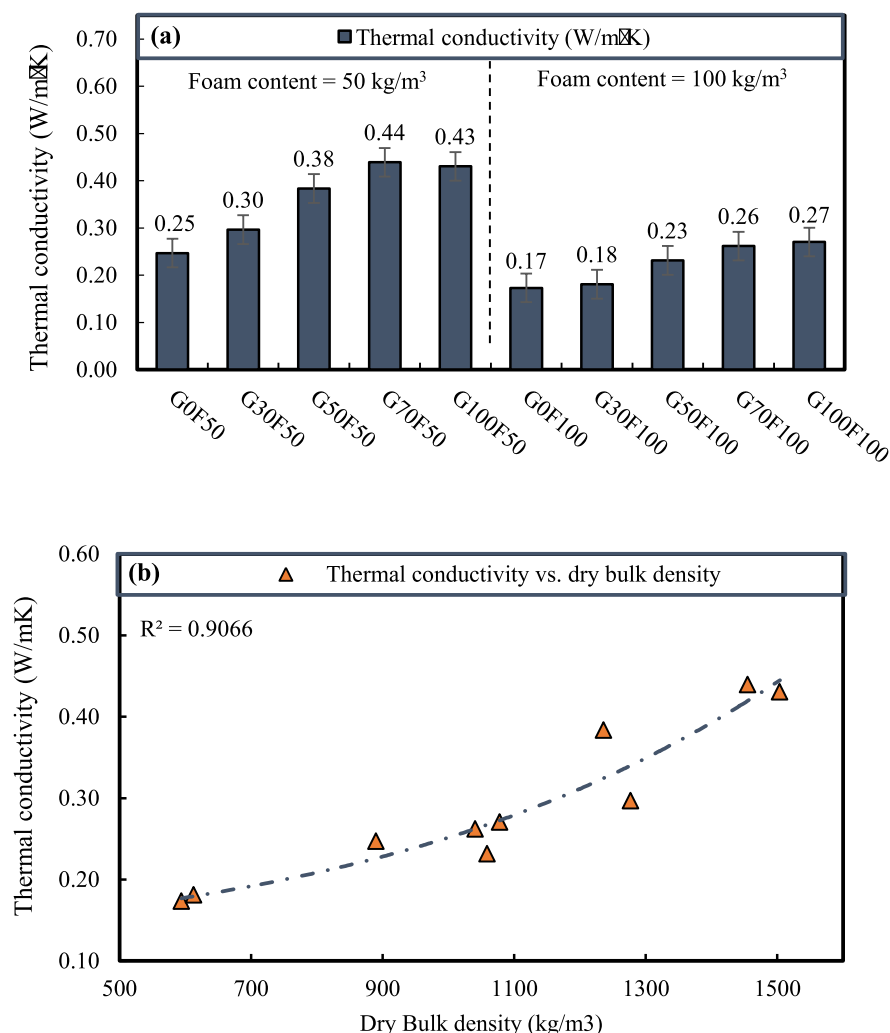
Thermal conductivity is one of the major properties through which one can measure the insulating degree of materials. It is commonly known that such insulating properties are mostly related to the porosity and bulk density of materials, which is adjustable in foam concretes [16]. Generally, an increase in the porosity results in an increase in the insulation properties of concrete. On this basis, foam concrete is well known to have a relatively less thermal conductivity due to its higher porosity than normal concrete.

Fig. 11(a) shows the results of thermal conductivity test conducted on different mixes after 28 days of curing. Based on the figure, thermal

conductivity of foam concretes ranged from 0.17 W/m.K for G0F100 to 0.44 W/m.K for G70F50. It can be seen in Fig. 11(a) that, as expected, mixes having a higher foam content exhibited a lower thermal conductivity (32–41%), which is owing to the higher content of solid materials in the matrix and less porous microstructure of the mixes with a less foam content [9,90]. As can also be seen in the figure, for a given foam content, an increased glass sand content caused an increased thermal conductivity of foam concrete. This observation agrees with the results of previous studies [91–94], and is owing to the higher specific gravity of glass sand compared to that of expanded perlite, as was shown in Table 2. Fig. 11(b) shows the relationship between thermal conductivity and dry bulk density of foam concrete in this study. According to this figure, increasing the dry bulk density caused an increased thermal conductivity of mixes, which is aligned with the results of previous studies [16,95].

### 3.11. Effect of high temperature and cooling regime

Since foam concrete is most commonly suitable for insulating applications, its resistance and stability to potential thermal stresses can provide further insight on the extent to which it can be used. In this study, two different cooling types of the heated mixes, including gradually air cooled and instantly cooled through immersion in water, have been adopted in accordance with previous studies ([96,97]).



**Fig. 11.** (a) Thermal conductivity of different mixes and (b) its relationship with dry bulk density.

### 3.11.1. Gradually air cooling

Figs. 12, 13, and 14 show the UPV variation, compressive strength, flexural strength, and mass loss of different mixes at 200, 400, 600, and 800 °C then cooled gradually in air at ambient temperature. As can be seen in Fig. 12, the UPV variation with respect to ambient temperature condition of air-cooled mixes ranged from + 5.54% for G100F100 at 200 °C to -55.95% for G0F50 at 800 °C. From Fig. 12, it is also evident that the exposure to high temperatures reduced the UPV speed of 50 kg/m<sup>3</sup> foam containing mixes more than their 100 kg/m<sup>3</sup> foam based companions. This shows the larger deteriorating effects of high temperature on 50 kg/m<sup>3</sup> foam containing mixes.

In addition, it can be seen that, for a given foam and glass sand content, an increase in the temperature led to a decrease in the UPV speed of foam concrete. However, it can be seen that an increased temperature to 200 °C led to a slight increase in the UPV speed of G100F50, GOF100, G30F100, and G100F100. As was reported in Ref. [98], this observation can be due to the continued hydration of unreacted particles in the foam concrete that takes place up to 200 °C. However, as was shown in Ref. [9], further increase in the temperature results in significant matrix disintegration, leading to UPV speed reduction.

Fig. 13(a) and (b) show the compressive and flexural strengths of different mixes after exposure to high temperatures then cooled gradually in air at ambient temperature, respectively. As can be seen in the

figures, the compressive strength of heated foam concretes ranged from 0.22 MPa (for G0F100 at 800 °C) to 4.92 MPa (for G70F50 at 200 °C), and their flexural strength ranged from 0 MPa (for G0F100 at 800 °C) to 0.92 MPa (for G100F50 at 200 °C). Based on the figures, for a given foam content and glass sand, an increase in the temperature caused a decrease in the compressive and flexural strengths of foam concrete. This observation is due to the induced thermal stress on specimens. As can be seen in Fig. 13(b), on average, the increase in foam content from 50 kg/m<sup>3</sup> to 100 kg/m<sup>3</sup> in mixes caused 80 and 56% compressive and flexural strengths reduction, respectively. In addition, mixes with 50 kg/m<sup>3</sup> and 100 kg/m<sup>3</sup> foam agent containing 100% glass sand and exposed to 800 °C exhibited ~ 79% higher compressive and ~ 66% flexural strength compared to the companion mixes containing 100% expanded perlite. The higher strength of mixes containing a higher glass sand content at high temperatures is due to the higher temperature resistance of glass compared to that of expanded perlite [16,29].

As can be seen in Fig. 14, the mass loss of heated foam concretes ranged from 0.20% (for G100F50 at 200 °C) to 14.97% (for G0F50 at 800 °C). According to the figure, for a given foam and glass sand content, increasing temperature led to an increase in the mass loss of foam concrete. This observation is because of the foam skeleton disintegration that takes place at higher temperatures [69]. An increased temperature from 200 to 800 °C in this study led to 476–2400% and 968–2558% increase in the mass loss of 50 and 100 kg/m<sup>3</sup> foam mixes, respectively,

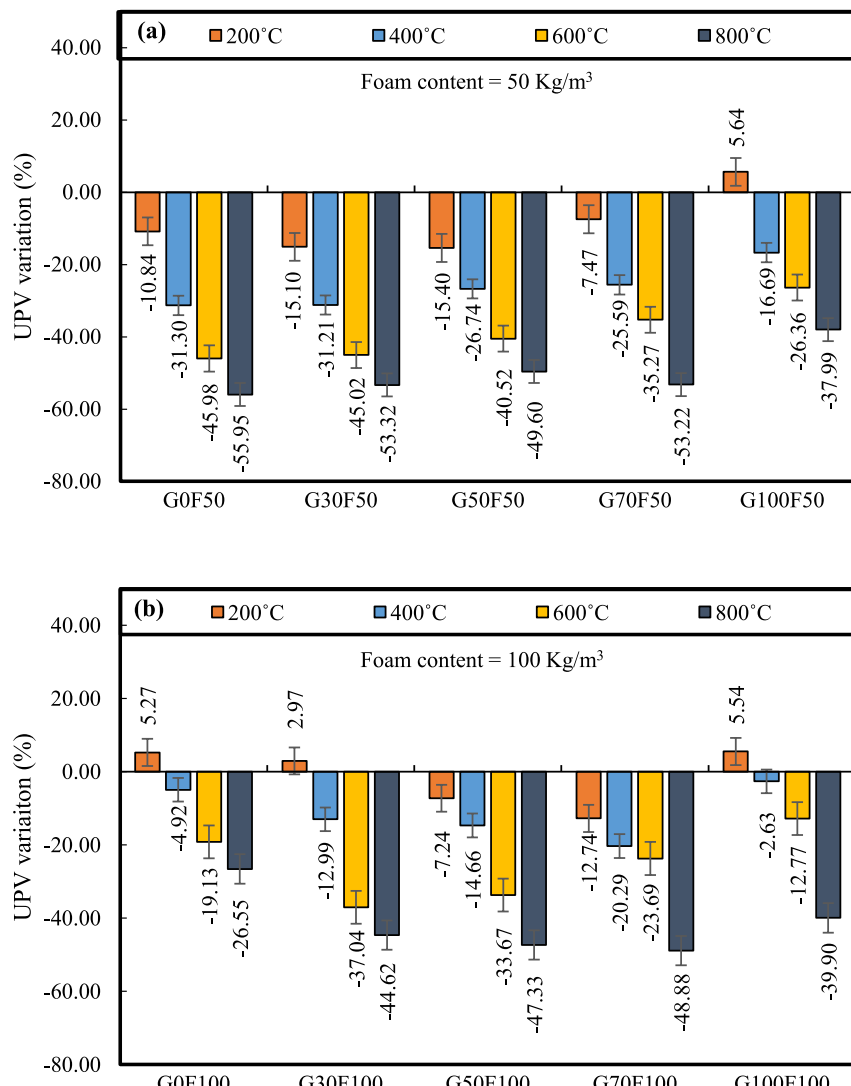


Fig. 12. UPV variation of heated and normally cooled mixes with foam content of (a) 50 kg/m<sup>3</sup> and (b) 100 kg/m<sup>3</sup>.

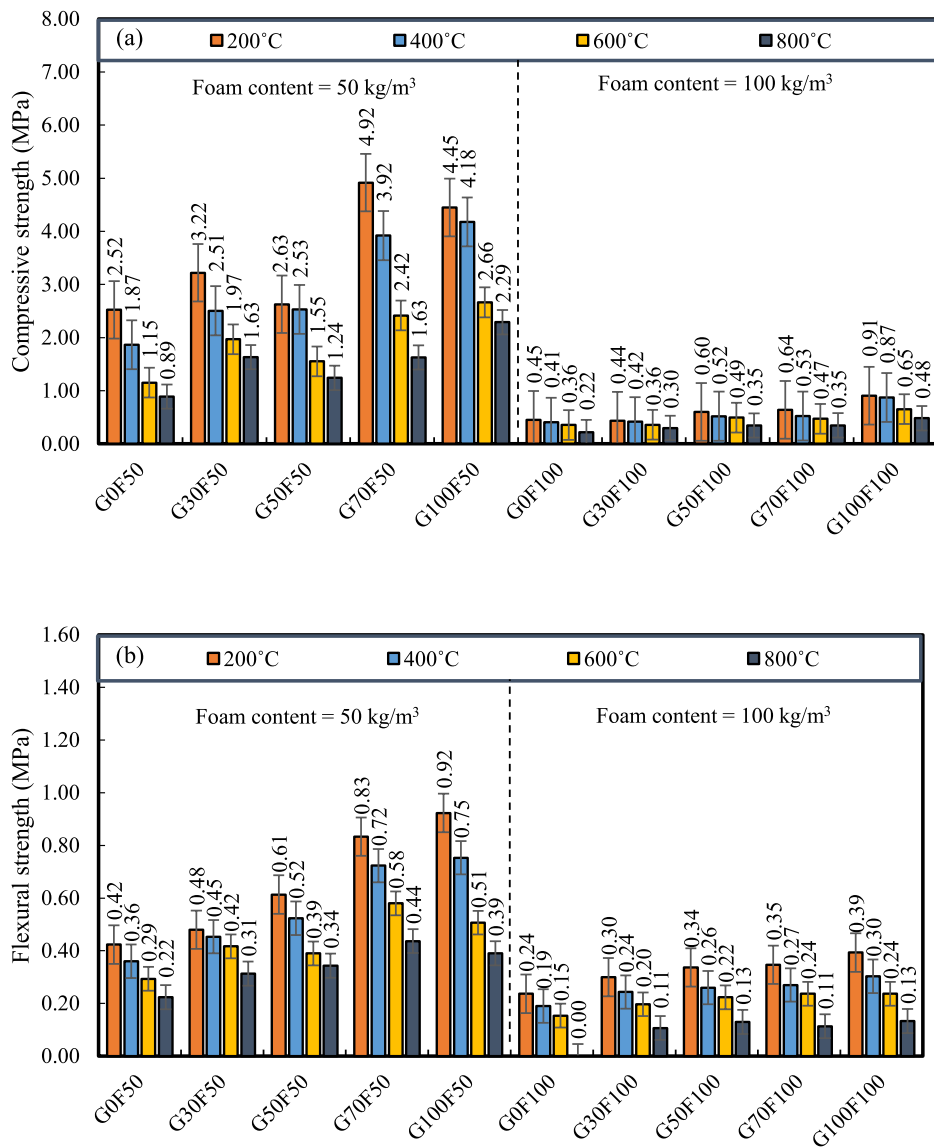


Fig. 13. (a) Compressive and (b) flexural strength test result of heated and normally cooled mixes.

indicating more significant mass loss in the foam mixes containing a higher foam content. This observation is consistent with previous studies [99,100] and is owing to higher thermal stress concentration on foam bubbles surfaces and the lower effects of aggregates to withstand this stress [8,101]. As can be observed in Fig. 14, for a given foam content and temperature, an increase in the glass sand content generally led to a decrease in the mass loss of foam concretes. This observation can be attributed to the higher strength of the mixes with an increased glass sand content at high temperatures owing to the higher melting point of glass compared to that of expanded perlite [16,29]. Further from Fig. 14, it can be seen that the mass loss of 100 kg/m<sup>3</sup> foam mixes was generally lower than that of 50 kg/m<sup>3</sup> foam mixes, which is different to the mass loss trend seen for freeze-thaw resistance (Fig. 10). This lower mass loss can be due to the higher insulation of 100 kg/m<sup>3</sup> foam containing mixes that is potentially resulted from higher porosity [16,17].

### 3.11.2. Instant cooling in water

Although cooling rate of heated mixes is not entertained numerously, the effect of cooling regime was reported to cause some variation in mechanical properties. According to Peng et al., [102], rapid cooling can cause a greater loss of compressive strength, splitting tensile strength, and fracture energy of concrete compared to gradual cooling. Gupta

et al., [103] attributed this larger loss to the wider cracks that appeared during rapid cooling.

Fig. 15 shows the UPV, compressive strength, and flexural strength of different heated mixes subjected to rapid cooling. As can be seen in the figure, at temperatures up to 200 °C, rapid cooling of 50 kg/m<sup>3</sup> foam mixes by immersion in water increased the compressive strength, and rapid cooling of 100 kg/m<sup>3</sup> foam mixes slightly decreased the compressive strength, potentially due to further hydration of materials when water cools the specimens [102,103]. In addition, comparing the results outlined in Fig. 12 with those in Fig. 15, it can be seen that, on average, in lower foam content mixes (50 kg/m<sup>3</sup>), air cooling resulted in lower UPV speed reduction while in mixes that had a higher foaming agent content (100 kg/m<sup>3</sup>), rapid cooling appeared to be more effective and had lower UPV speed reduction.

Based on the results of this study, the compressive and flexural strengths reductions of rapid cooled mixes (reduction from 200 °C to 800 °C) were ~ 60% and ~ 52% compared to those of the unheated mixes, respectively. In addition, the compressive and flexural strengths reductions of rapid cooled mixes were ~ 6% higher and ~ 3% lower compared to those of companion gradual cooled mixes, respectively. This observation conforms to the results presented by Refs. [96,102,103].

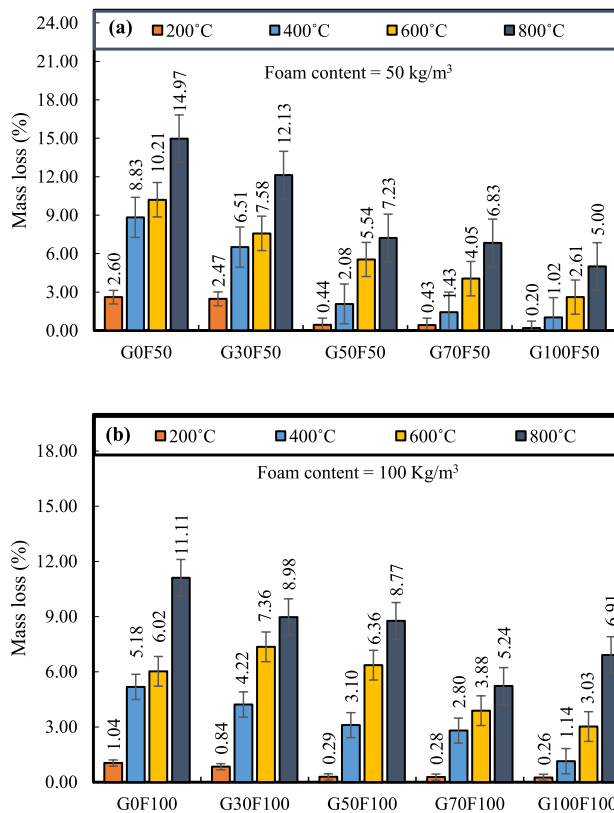


**Fig. 14.** Mass loss of different mixes subjected to high temperatures: foam content of (a) 50 kg/m<sup>3</sup> and (b) 100 kg/m<sup>3</sup>.

### 3.12. SEM / EDS analysis

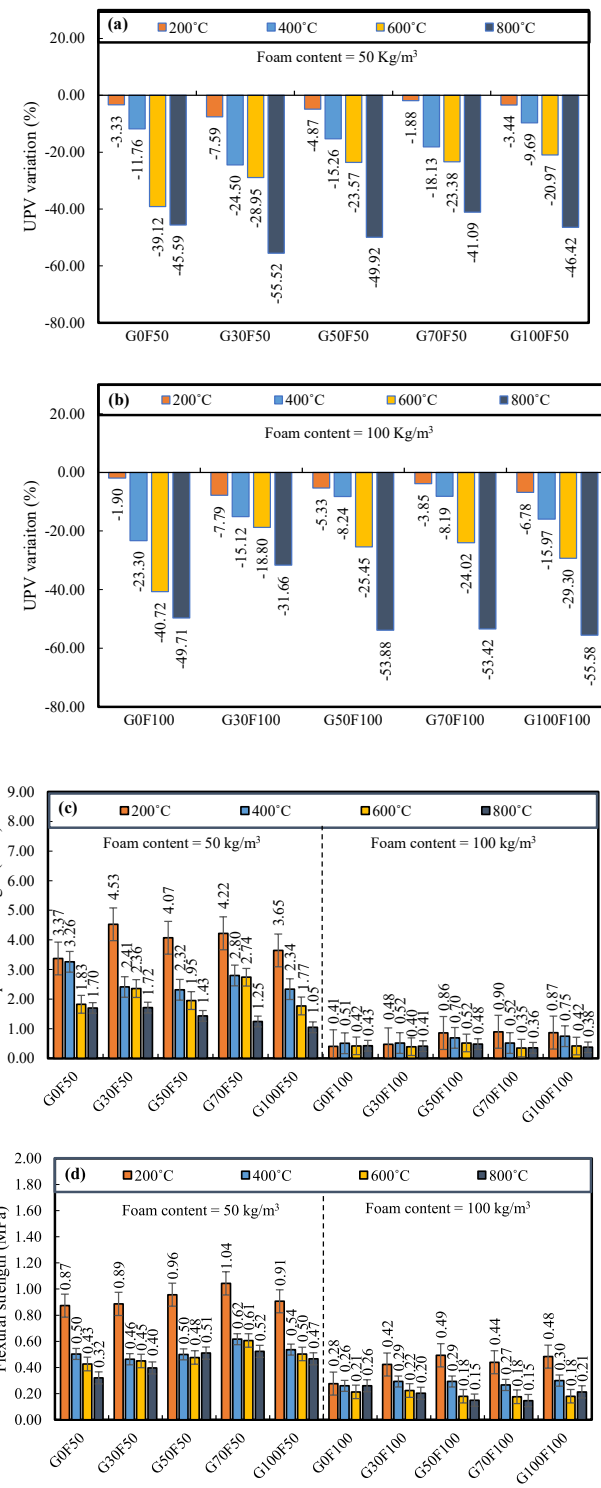
#### 3.12.1. SEM / EDS of foam concrete after ASR

Arguably, scanning electron microscopy (SEM) and energy dispersive spectroscopy (EDS) are two of the most useful characterization tools providing visual and chemical compositional details of concrete materials. Fig. 16 shows the SEM images of G0F100, G50F50 and G100F100 after 25 cycles of ASR. Based on the figure, it is evident that in almost all mixes certain cracks were developed when they were exposed to ASR cycle. Yet, the cracks in G0F100 (shown in Fig. 16(a) and (b)) appeared to have a larger width compared to those in G50F50 (shown in Fig. 16(c) and (d)) and G100F100 (shown in Fig. 16(e) and (f)). According to Figs. 16(c)–(f), G50F50 had a larger number of microcracks with larger width compared to G100F100. These observations can explain why an increased glass sand caused a decrease in the ASR expansion of foam concrete. This can be due to the lower strength of expanded perlite aggregates in withstanding internal stresses caused by ASR cycle compared to that of glass sand [29,92].

Table 7 shows the results of EDS conducted on G0F100, G50F50 and G100F100. As can be seen, mixes having a higher content of glass sand had a higher content of calcium, a lower content of aluminum, and almost similar content of silicon. Based on the table, the calcium content of G0F100 was 15.38% (by weight), while that of G50F50 and G100F100 was 22.63% and 34.53%, respectively. Therefore, mixes with 100% glass sand had almost twice calcium content in their matrix compared to those with 0% glass sand. This observation indicates that the foam mixes with a higher glass sand content had more hydration product of calcium silicate hydrate (C-S-H) in their microstructure compared to those with a lower glass sand content, which matches with the observation of SEM images in Fig. 16.

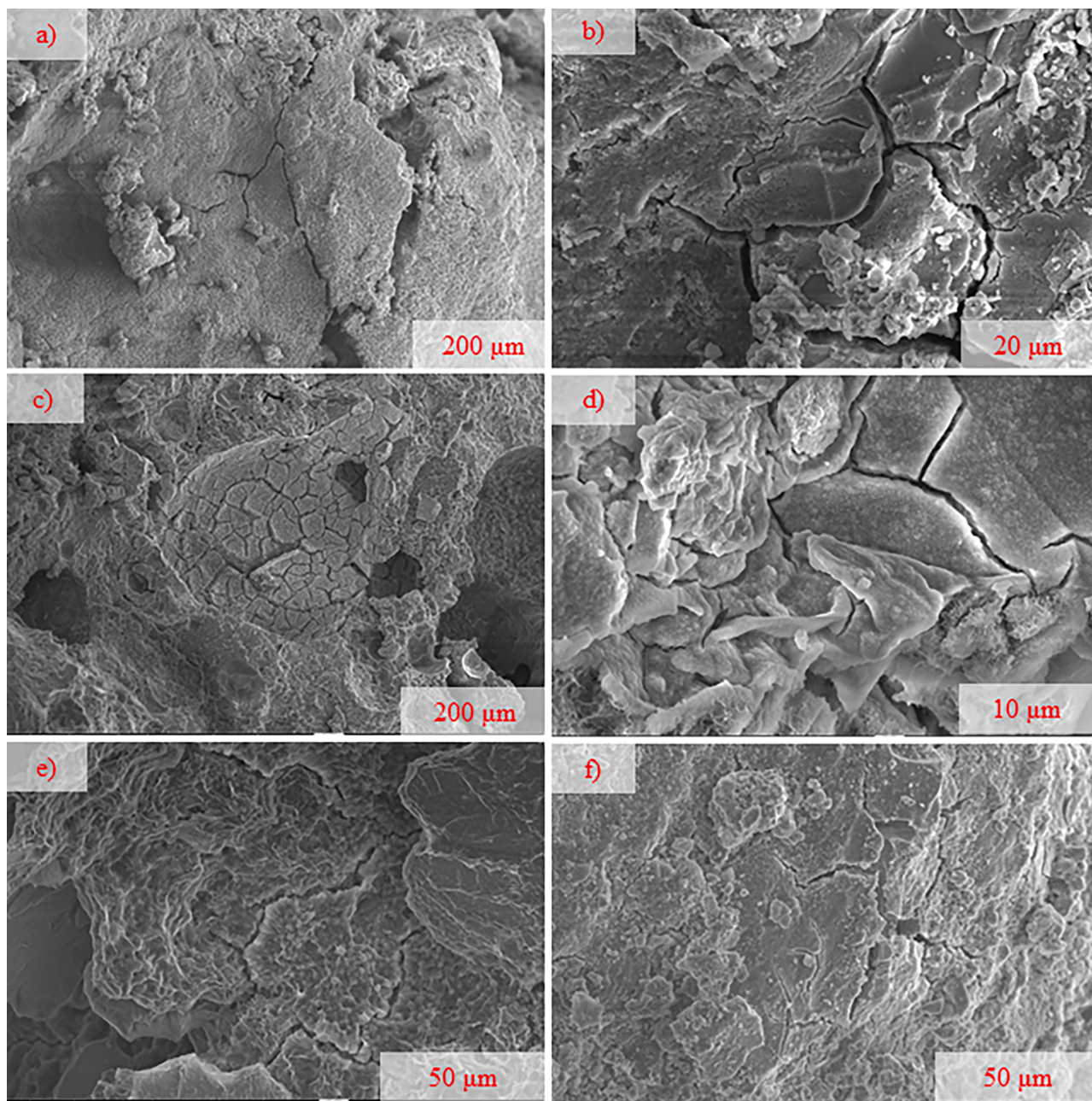
#### 3.12.2. SEM / EDS of foam concrete under high temperatures

Fig. 17 shows the SEM images taken from G0F100, G50F50 and



**Fig. 15.** The effect of rapid cooling on (a) UPV reduction of mixes with foam content of 50 kg/m<sup>3</sup>, (b) UPV reduction of mixes with foam content of 100 kg/m<sup>3</sup>, (c) compressive strength of different mixes, and (d) flexural strength of different mixes.

G100F100 heated at 800°C. Fig. 17(a) and (b) present the SEM images of G0F100 rapidly cooled in water, while Fig. 17(c) and (d) and Fig. 17(e) and (f) present the SEM images of G50F50 and G100F100 gradually cooled in ambient temperature, respectively. Based on the figures, almost all mixes developed microcracks within their microstructure as a result of high temperature exposure. As can be seen from the figures, the cracks appeared to have been marginally healed in the rapidly cooled



**Fig. 16.** Low- and high-magnification SEM images of (a and b) GOF100, (c and d) G50F50 and (e and f) G100F100.

**Table 7**  
EDS (weight %) of GOF100, G50F50 and G100F100.

Specimen	O	Na	Mg	Al	Si	S	K	Ca	Fe
GOF100	39.12	11.6	0.01	2.47	15.31	1.51	1.23	15.38	1.81
G50F50	42.5	13.21	0.16	1.5	15.78	1.72	1.76	22.63	0.74
G100F100	44.64	6.06	0.44	0.8	10.75	0.94	0.12	34.53	1.7

specimen (GOF100). This observation can also be confirmed by Table 8, which shows the EDS of the same mixes. Based on the table, the rapidly water-cooled mix of GOF100 had the highest degree of calcium content (48.75%) compared to gradually cooled mixes of G50F50 (35.71%) and G100F100 (35.15%). It can also be seen when comparing Tables 7 and 8 that heated mixes consumed most of their Na content while a large increase in the available calcium content is observed. In this analysis, it appears that the rapidly cooled water developed a significantly larger

calcium content when compared to gradually cooled mixes. In this regard, further microstructural studies in this area can provide further insight on the mechanism through which gradual cooling and rapid cooling affect the microstructure of the mixes.

#### 4. Conclusions

In this study, the effect of two different quantities of foaming agent

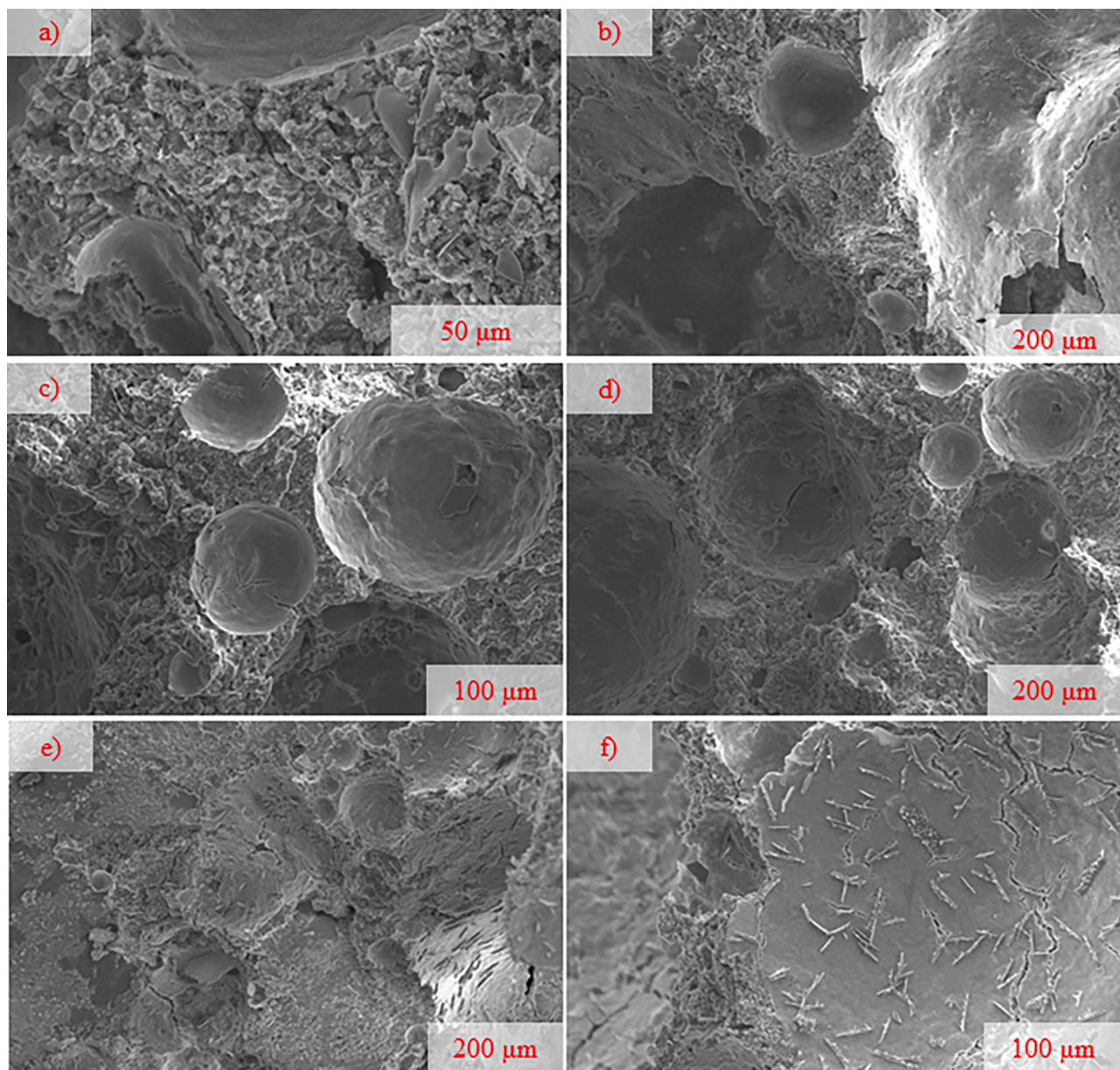


**Fig. 17.** Low- and high-magnification SEM images of different mixes heated at 800 °C: (a and b) GOF100 rapidly cooled in water, (c and d) G50F50 gradually cooled in air, and (e and f) G100F100 gradually cooled in air.

**Table 8**

EDS (by weight %) of GOF100, G50F50 and G100F100 heated at 800 °C with different cooling conditions of rapid water cooling (GOF100) and gradual air cooling (G50F50 and G100F100).

Specimen	O	Na	Mg	Al	Si	S	K	Ca	Fe
GOF100	30.1	0.04	0	1.67	10.03	2.21	1.17	48.75	6.03
G50F50	40.74	1.5	0.49	2.57	12.19	2.16	1.5	35.71	3.14
G100F100	52.88	0.88	0.28	1.07	8.22	0.89	0	35.15	0.64

(50 and 100 kg/m<sup>3</sup>) in addition to the replacement (0, 30, 50, 70, and 100%) of lightweight expanded perlite with waste glass sand has been exercised. Based on the results of this study, the following conclusions can be drawn:

- An increase in the glass sand content leads to an increase in the flowability of foam concrete at a given foam content. This can potentially be associated with the smooth surface and impermeability of glass particles.

- The addition of glass sand increases the compressive and flexural strengths of foam concrete for a given foam content and curing age. In the same fashion, the addition of glass sand has a more positive effect on the strength development of the foam concrete with a lower content of foam agent, which can be due to the better surface adhesion of the glass sand with paste matrix in a less porous mix.
- For a given foam content, the addition of glass sand increases the bulk density and decreases the apparent porosity, water absorption and sorptivity of foam concrete, with a more significant influences on

- the concrete with a lower foam content. This observation can be because of the higher specific gravity and less water absorption of glass sand compared to those of expanded perlite.
- Although previous studies have noted a higher drying shrinkage (up to 5 to 10 times) for foam concrete compared to that of normal concrete, the results of this study showed that such high drying shrinkages can be significantly reduced by the addition of glass sand. This can be mainly associated with enhanced ability of concrete containing glass to withstand internal stress caused by drying shrinkage. Additionally, since glass particles have a smooth surface with a considerably low porosity, they can further avoid drying shrinkage potentials.
  - The use of glass sand in fine sizes (e.g., < 2.36 mm) decreases the ASR expansion of foam concrete by up to 38%. Notably, the early expansion rate of concretes with 100% glass sand decreases by up to 60%. Such enhanced effects have further been supported by the higher calcium content found through EDS in concretes containing a higher glass sand content.
  - The result of freeze-thaw resistance test showed that foam concretes containing a higher degree of glass sand experience significantly less mass loss. In essence, this can be attributed to the significantly lower porosity of glass sand compared to that of expanded perlite.
  - The results of thermal conductivity and thermal resistance tests showed that a higher foam content results in a lower mass loss and conductivity, which become offset by the addition of glass sand mostly due to the decreased porosity of the foam concrete with an increased glass sand. These results show the high effectiveness of glass sand at high temperatures, due to its high melting point.
  - The results of this study showed that cooling regime can result in a slightly lowered strength reduction after thermal exposure, potentially due to the effect of sudden temperature change. The results of SEM / EDS analysis, however, showed that rapid cooled concretes have a higher calcium content in their microstructure. It is recommended to further investigate the chemical transformation of foam concretes under different cooling regimes.

According to the results of this study, the best overall performing foam concrete mix was the mix containing 50 kg/m<sup>3</sup> foaming agent, 70% glass sand and 30% expanded perlite aggregate. However, further studies are recommended to design the mix according to the required strength and properties.

#### CRediT authorship contribution statement

**Osman Gencel:** Supervision, Project administration, Methodology, Resources, Investigation, Conceptualization. **Oguzhan Yavuz Bayraktar:** Project administration, Data curation, Resources, Investigation. **Gokhan Kaplan:** Project administration, Data curation, Resources, Investigation. **Oguz Arslan:** Project administration, Data curation, Resources, Investigation. **Mehrab Nodehi:** Writing – original draft, Writing – review & editing, Visualization, Validation. **Ahmet Benli:** Data curation, Resources, Investigation. **Aliakbar Gholampour:** Writing – review & editing, Validation. **Togay Ozbakkaloglu:** Supervision, Project administration, Methodology, Writing – review & editing.

#### Declaration of Competing Interest

The authors declare that they have no known competing financial interests or personal relationships that could have appeared to influence the work reported in this paper.

#### Acknowledgement

The authors appreciate and acknowledge the support received from the Universities of Bartin, Kastamonu, Erzurum and Bingol during the development of this study.

#### References

- [1] F. Krausmann, S. Gingrich, N. Eisenmenger, K.H. Erb, H. Haberl, M. Fischer-Kowalski, Growth in global materials use, GDP and population during the 20th century, *Ecol. Econ.* 68 (10) (2009) 2696–2705, <https://doi.org/10.1016/j.ecolecon.2009.05.007>.
- [2] O. Ortiz, F. Castells, G. Sonnemann, Sustainability in the construction industry: A review of recent developments based on LCA, *Constr. Build. Mater.* 23 (1) (2009) 28–39, <https://doi.org/10.1016/j.conbuildmat.2007.11.012>.
- [3] X. Zhao, B.-G. Hwang, J. Lim, Job satisfaction of project managers in green construction projects: constituents, barriers, and improvement strategies, *J. Clean. Prod.* 246 (2020) 118968, <https://doi.org/10.1016/j.jclepro.2019.118968>.
- [4] J. Lehne, F. Preston, Chatham house report making concrete change innovation in low-carbon cement and concrete the royal institute of international affairs, chatham house report series, [www.chathamhouse.org/sites/default/files/publications/research/2018-06/13-makingconcrete- c](http://www.chathamhouse.org/sites/default/files/publications/research/2018-06/13-makingconcrete- c), 2018.
- [5] A. Arrigoni, D.K. Panesar, M. Duhamel, T. Opher, S. Saxe, I.D. Posen, H. L. MacLean, Life cycle greenhouse gas emissions of concrete containing supplementary cementitious materials: cut-off vs. substitution, *J. Clean. Prod.* 263 (2020) 121465, <https://doi.org/10.1016/j.jclepro.2020.121465>.
- [6] R. Snellings, Assessing, understanding and unlocking supplementary cementitious materials, *RILEM Tech. Lett.* 1 (2016) 50, <https://doi.org/10.21809/rilemttechlett.2016.12>.
- [7] M. Sandanayake, W. Lokuge, G. Zhang, S. Setunge, and Q. Thushar, Greenhouse gas emissions during timber and concrete building construction —A scenario based comparative case study, *Sustain. Cities Soc.*, vol. 38, no. August 2017, pp. 91–97, 2018, doi: 10.1016/j.scs.2017.12.017.
- [8] A. Raj, D. Sathyam, K.M. Mini, Physical and functional characteristics of foam concrete: A review, *Constr. Build. Mater.* 221 (2019) 787–799, <https://doi.org/10.1016/j.conbuildmat.2019.06.052>.
- [9] O. Gencel, A. Benli, O.Y. Bayraktar, G. Kaplan, M. Sutcu, W.A.T. Elabade, Effect of waste marble powder and rice husk ash on the microstructural, physico-mechanical and transport properties of foam concretes exposed to high temperatures and freeze-thaw cycles, *Constr. Build. Mater.* 291 (2021) 123374, <https://doi.org/10.1016/j.conbuildmat.2021.123374>.
- [10] R. C. Valore, *Foam and gas concretes*, 1961.
- [11] Z. Zhang, J.L. Provis, A. Reid, H. Wang, Geopolymer foam concrete: An emerging material for sustainable construction, *Constr. Build. Mater.* 56 (2014) 113–127, <https://doi.org/10.1016/j.conbuildmat.2014.01.081>.
- [12] I. K. Harith, Study on polyurethane foamed concrete for use in structural applications, *Case Stud. Constr. Mater.*, vol. 8, no. November 2017, pp. 79–86, 2018, doi: 10.1016/j.cscm.2017.11.005.
- [13] M.R. Jones, L. Zheng, K. Ozlutas, Stability and instability of foamed concrete, *Mag. Concr. Res.* 68 (11) (2016) 542–549, <https://doi.org/10.1680/macr.15.00097>.
- [14] A.L. Fameau, A. Salonen, Effect of particles and aggregated structures on the foam stability and aging, *Comptes Rendus Phys.* 15 (8–9) (2014) 748–760, <https://doi.org/10.1016/j.crhy.2014.09.009>.
- [15] K. DhasindraKrishna, K. Pasupathy, S. Ramakrishnan, J. Sanjayan, Effect of yield stress development on the foam-stability of aerated geopolymers concrete, *Cem. Concr. Res.* 138 (2020) 106233, <https://doi.org/10.1016/j.cemconres.2020.106233>.
- [16] M. Nodehi, A comparative review on foam-based versus lightweight aggregate-based alkali-activated materials and geopolymers, *Innov. Infrastruct. Solut.* 6 (4) (Dec. 2012) 231, <https://doi.org/10.1007/s41062-021-00595-w>.
- [17] K. DhasindraKrishna, K. Pasupathy, S. Ramakrishnan, J. Sanjayan, Progress, current thinking and challenges in geopolymers foam concrete technology, *Cem. Compos.* 116 (November) (2021) 103886, <https://doi.org/10.1016/j.cemconcomp.2020.103886>.
- [18] S. Onutai, S. Jimsirilars, P. Thavornmiti, T. Kobayashi, Fast microwave syntheses of fly ash based porous geopolymers in the presence of high alkali concentration, *Ceram. Int.* 42 (8) (2016) 9866–9874, <https://doi.org/10.1016/j.ceramint.2016.03.086>.
- [19] Y.C. Ersan, S. Gulcimen, T.N. Imis, O. Saygin, N. Uzal, Life cycle assessment of lightweight concrete containing recycled plastics and fly ash, *Eur. J. Environ. Civ. Eng.* (2020) 1–14, <https://doi.org/10.1080/19648189.2020.1767216>.
- [20] O. Gencel, M. Oguz, A. Gholampour, T. Ozbakkaloglu, Recycling waste concretes as fine aggregate and fly ash as binder in production of thermal insulating foam concretes, *J. Build. Eng.* 38 (November) (2021) 102232, <https://doi.org/10.1016/j.jobe.2021.102232>.
- [21] B. Coppola, L. Courard, F. Michel, L. Incarnato, L. Di Maio, Investigation on the use of foamed plastic waste as natural aggregates replacement in lightweight mortar, *Compos. Part B Eng.* 99 (2016) 75–83, <https://doi.org/10.1016/j.compositesb.2016.05.058>.
- [22] I. Turkmen, A. Kantarci, Effects of expanded perlite aggregate and different curing conditions on the physical and mechanical properties of self-compacting concrete, *Build. Environ.* 42 (6) (2007) 2378–2383, <https://doi.org/10.1016/j.buildenv.2006.06.002>.
- [23] S. Sharook, D. Sathyam, M.K. Madhavan, Thermo-mechanical and durability properties of expanded perlite aggregate foamed concrete, *Proc. Inst. Civ. Eng. - Constr. Mater.* (2020) 1–9, <https://doi.org/10.1680/jcoma.20.00041>.
- [24] R. T. Sataloff, M. M. Johns, K. M. Kost, Advanced concrete technology.
- [25] J.Y. Yoon, J.H. Kim, Y.Y. Hwang, D.K. Shin, Lightweight concrete produced using a two-stage casting process, *Materials (Basel)* 8 (4) (2015) 1384–1397, <https://doi.org/10.3390/ma8041384>.

- [26] I.B. Topçu, M. Canbaz, Properties of concrete containing waste glass, *Cem. Concr. Res.* 34 (2) (2004) 267–274, <https://doi.org/10.1016/j.cemconres.2003.07.003>.
- [27] A. Omran, A. Tagnit-Hamou, Performance of glass-powder concrete in field applications, *Constr. Build. Mater.* 109 (2016) 84–95, <https://doi.org/10.1016/j.conbuildmat.2016.02.006>.
- [28] W. Dong, Y. Guo, Z. Sun, Z. Tao, W. Li, Development of piezoresistive cement-based sensor using recycled waste glass cullets coated with carbon nanotubes, *J. Clean. Prod.* 314 (2021) 127968, <https://doi.org/10.1016/j.jclepro.2021.127968>.
- [29] M. Nodehi and V. Mohamad Taghvaei, Sustainable concrete for circular economy: a review on use of waste glass, *Glas. Struct. Eng.*, May 2021, doi: 10.1007/s40940-021-00155-9.
- [30] P. Guo, W. Meng, H. Nassif, H. Gou, Y. Bao, New perspectives on recycling waste glass in manufacturing concrete for sustainable civil infrastructure, *Constr. Build. Mater.*, vol. 257, p. 119579, 2020, doi: 10.1016/j.conbuildmat.2020.119579.
- [31] O.M. Olofinnade, A.N. Ede, J.M. Ndambuki, B.U. Ngene, I.I. Akinwumi, O. Ofuyatan, S.K. Shukla, Strength and microstructure of eco-concrete produced using waste glass as partial and complete replacement for sand, *Cogent Eng.* 5 (1) (2018) 1483860, <https://doi.org/10.1080/23311916.2018.1483860>.
- [32] A.W. Larsen, H. Merrild, T.H. Christensen, Recycling of glass: Accounting of greenhouse gases and global warming contributions, *Waste Manag. Res.* 27 (8) (2009) 754–762, <https://doi.org/10.1177/0734242X09342148>.
- [33] A. Schmitz, J. Kamiński, B. Maria Scalet, A. Soria, Energy consumption and CO<sub>2</sub> emissions of the European glass industry, *Energy Policy* 39 (1) (2011) 142–155, <https://doi.org/10.1016/j.enpol.2010.09.022>.
- [34] H. Zhu, W. Chen, W. Zhou, E.A. Byars, Expansion behaviour of glass aggregates in different testing for alkali-silica reactivity, *Mater. Struct. Constr.* 42 (4) (2009) 485–494, <https://doi.org/10.1617/s11527-008-9396-4>.
- [35] S. Yang, H. Cui, C. S. Poon, Assessment of in-situ alkali-silica reaction (ASR) development of glass aggregate concrete prepared with dry-mix and conventional wet-mix methods by X-ray computed micro-tomography, vol. 90, no. April, pp. 266–276, 2018, doi: 10.1016/j.cemconcomp.2018.03.027.
- [36] W. Dong, W. Li, Z. Tao, A comprehensive review on performance of cementitious and geopolymeric concretes with recycled waste glass as powder, sand or cullet, *Resources, Conservation and Recycling*, vol. 172, no. April. Elsevier B.V., p. 105664, 2021, <https://doi.org/10.1016/j.resconrec.2021.105664>.
- [37] S.B. Park, B.C. Lee, J.H. Kim, Studies on mechanical properties of concrete containing waste glass aggregate, *Cem. Concr. Res.* 34 (12) (2004) 2181–2189, <https://doi.org/10.1016/j.cemconres.2004.02.006>.
- [38] Z.Z. Ismail, E. A. Al-Hashmi, Recycling of waste glass as a partial replacement for fine aggregate in concrete, *Waste Manag.* 29 (2) (2009) 655–659, <https://doi.org/10.1016/j.wasman.2008.08.012>.
- [39] K. Afshinnia, P.R. Rangaraju, Influence of fineness of ground recycled glass on mitigation of alkali-silica reaction in mortars, *Constr. Build. Mater.* 81 (2015) 257–267, <https://doi.org/10.1016/j.conbuildmat.2015.02.041>.
- [40] V. Corinaldesi, G. Gnappi, G. Moriconi, A. Montenero, Reuse of ground waste glass as aggregate for mortars, *Waste Manag.* 25 (2) (2005) 197–201, <https://doi.org/10.1016/j.wasman.2004.12.009>.
- [41] H. Du, K.H. Tan, Effect of particle size on alkali-silica reaction in recycled glass mortars, *Constr. Build. Mater.* 66 (2014) 275–285, <https://doi.org/10.1016/j.conbuildmat.2014.05.092>.
- [42] Q.S. Khan, M.N. Sheikh, T.J. McCarthy, M. Robati, M. Allen, Experimental investigation on foam concrete without and with recycled glass powder: A sustainable solution for future construction, *Constr. Build. Mater.* 201 (2019) 369–379, <https://doi.org/10.1016/j.conbuildmat.2018.12.178>.
- [43] K. Schumacher, N. Saßmannshausen, C. Pritzel, R. Trettin, Lightweight aggregate concrete with an open structure and a porous matrix with an improved ratio of compressive strength to dry density, *Constr. Build. Mater.* 264 (2020) 120167, <https://doi.org/10.1016/j.conbuildmat.2020.120167>.
- [44] ASTM, ASTM - C869-91 Standard Specification for Foaming Agents Used in Making Preformed Foam for, Cellular Concrete 80 (2011) (2011) 1–2, <https://doi.org/10.1520/C0869>.
- [45] O. Yavuz Bayraktar, G. Kaplan, O. Gencel, A. Benli, M. Sutcu, Physico-mechanical, durability and thermal properties of basalt fiber reinforced foamed concrete containing waste marble powder and slag, *Constr. Build. Mater.* 288 (2021) 123128, <https://doi.org/10.1016/j.conbuildmat.2021.123128>.
- [46] ASTM, C230, Standard specification for flow table for use in tests of hydraulic cement, Annu. B. ASTM Stand. (2010) 4–9, <https://doi.org/10.1520/C0230>.
- [47] ASTM C29/C29M-09, Standard Test Method for Bulk Density (' Unit Weight ') and Voids in Aggregate, ASTM Int., vol. i, no. c, pp. 1–5, 2009, doi: 10.1520/C0029.
- [48] ASTM C20-15, Standard Test Methods for Apparent Porosity, Water Absorption, Apparent Specific Gravity, and Bulk Density of Burned Refractory Brick and Shapes by Boiling Water, 2015, doi: 10.1520/C0020-00R15.
- [49] ASTM, C948, Standard Test method for dry and wet bulk density, water absorption, and apparent porosity of thin sections of glass-fiber reinforced concrete, *ASTM Int.* 81 (August) (2016) 1981, p. 2, <https://doi.org/10.1520/C0948-81R16.1>.
- [50] ASTM, C1585-13, Standard test method for measurement of rate of absorption of water by hydraulic cement concretes, *ASTM Int.* 41 (147) (2013) 1–6, <https://doi.org/10.1520/C1585-13.2>.
- [51] ASTM C349-08, Standard test method for compressive strength of hydraulic-cement mortars (using portions of prisms broken in flexure), ASTM International, pp. 1–4, 2008, doi: 10.1520/C0349-14.2.
- [52] ASTM, C348, Standard Test Method for Flexural Strength of Hydraulic-Cement Mortars, Annu. B. ASTM Stand. 04 (2014) 2–7, <https://doi.org/10.1520/C0348-14.2>.
- [53] ASTM C, 596–01, Standard Test Method for Drying Shrinkage of Mortar Containing Hydraulic Cement, Annu. B. ASTM Stand. 2 (4) (2001) 11–13, <https://doi.org/10.1520/C0596-09>.
- [54] ASTM C666/C666M, Standard Test Method for Resistance of Concrete to Rapid Freezing and Thawing, ASTM Int. West Conshohocken, PA, vol. 03, no. Reapproved, pp. 1–6, 2003, doi: 10.1520/C0666.
- [55] ASTM, C227, Standard Test Method for Potential Alkali Reactivity of Cement-Aggregate Combinations (Mortar-Bar Method), Annu. B. ASTM Stand. (2003) 1–5, <https://doi.org/10.1520/C1260-14.2>.
- [56] H. Du, K.H. Tan, Properties of high volume glass powder concrete, *Cem. Concr. Compos.* 75 (2017) 22–29, <https://doi.org/10.1016/j.cemconcomp.2016.10.010>.
- [57] A.A. Aliabdo, A.E.M. Abd Elmoaty, A.Y. Aboshama, Utilization of waste glass powder in the production of cement and concrete, *Constr. Build. Mater.* 124 (2016) 866–877, <https://doi.org/10.1016/j.conbuildmat.2016.08.016>.
- [58] H.A. Elaqra, M.A.A. Haloub, R.N. Rustom, Effect of new mixing method of glass powder as cement replacement on mechanical behavior of concrete, *Constr. Build. Mater.* 203 (2019) 75–82, <https://doi.org/10.1016/j.conbuildmat.2019.01.077>.
- [59] S.C. Kou, C.S. Poon, Properties of self-compacting concrete prepared with recycled glass aggregate, *Cem. Concr. Compos.* 31 (2) (2009) 107–113, <https://doi.org/10.1016/j.cemconcomp.2008.12.002>.
- [60] E.K. Kunhanandan Nambiar, K. Ramamurthy, Fresh state characteristics of foam concrete, *J. Mater. Civ. Eng.* 20 (2) (2008) 111–117, [https://doi.org/10.1061/\(asce\)0899-1561\(2008\)20:2\(111\)](https://doi.org/10.1061/(asce)0899-1561(2008)20:2(111)).
- [61] P. Stevenson, *Foam engineering*, John Wiley & Sons Ltd, Chichester, UK, 2012.
- [62] E. Kuzielová, L. Pach, M. Palou, Effect of activated foaming agent on the foam concrete properties, *Constr. Build. Mater.* 125 (2016) 998–1004, <https://doi.org/10.1016/j.conbuildmat.2016.08.122>.
- [63] S. Varghese, A. M. Ashok, A. K. Joseph, S. Emmanuel, O. V Swathylekshmi, A study on properties of foamed concrete with natural and synthetic foaming agent, *Int. Res. J. Eng. Technol.*, vol. 4, no. 3, pp. 2009–2011, 2017, [Online]. Available: <https://irjet.net/archives/V4/I3/IRJET-V4I3534.pdf>.
- [64] A. Mohajerani, J. Vajna, T.H.H. Cheung, H. Kurmus, A. Arulrajah, S. Horpibulsuk, Practical recycling applications of crushed waste glass in construction materials: A review, *Constr. Build. Mater.* 156 (2017) 443–467, <https://doi.org/10.1016/j.conbuildmat.2017.09.005>.
- [65] A.M. Rashad, A synopsis about perlite as building material - A best practice guide for Civil Engineer, *Constr. Build. Mater.* 121 (2016) 338–353, <https://doi.org/10.1016/j.conbuildmat.2016.06.001>.
- [66] O. Gencel, O. Yavuz Bayraktar, G. Kaplan, A. Benli, G. Martínez-Barrera, W. Brostow, M. Tek, B. Bodur, Characteristics of hemp fibre reinforced foam concretes with fly ash and Taguchi optimization, *Constr. Build. Mater.* 294 (2021) 123607, <https://doi.org/10.1016/j.conbuildmat.2021.123607>.
- [67] E.K.K. Nambiar, K. Ramamurthy, Air-void characterisation of foam concrete, *Cem. Concr. Res.* 37 (2) (2007) 221–230, <https://doi.org/10.1016/j.cemconres.2006.10.009>.
- [68] E.P. Kearsley, P.J. Wainwright, The effect of porosity on the strength of foamed concrete, *Cem. Concr. Res.* 32 (2) (2002) 233–239, [https://doi.org/10.1016/S0008-8846\(01\)00665-2](https://doi.org/10.1016/S0008-8846(01)00665-2).
- [69] K. Ramamurthy, E. K. Kunhanandan Nambiar, G. Indu Siva Ranjani, A classification of studies on properties of foam concrete, *Cem. Concr. Compos.*, vol. 31, no. 6, pp. 388–396, 2009, doi: 10.1016/j.cemconcomp.2009.04.006.
- [70] R. Nemes, Z. Józsa, Strength of lightweight glass aggregate concrete, *J. Mater. Civ. Eng.* 18 (5) (2006) 710–714, [https://doi.org/10.1061/\(asce\)0899-1561\(2006\)18:5\(710\)](https://doi.org/10.1061/(asce)0899-1561(2006)18:5(710)).
- [71] R.U.D. Nassar, P. Sorourshian, Strength and durability of recycled aggregate concrete containing milled glass as partial replacement for cement, *Constr. Build. Mater.* 29 (2012) 368–377, <https://doi.org/10.1016/j.conbuildmat.2011.10.061>.
- [72] K. Ganeshan, K. Rajagopal, K. Thangavel, Rice husk ash blended cement: assessment of optimal level of replacement for strength and permeability properties of concrete, *Constr. Build. Mater.* 22 (8) (2008) 1675–1683, <https://doi.org/10.1016/j.conbuildmat.2007.06.011>.
- [73] A. Saccani, M.C. Bignozzi, ASR expansion behavior of recycled glass fine aggregates in concrete, *Cem. Concr. Res.* 40 (4) (2010) 531–536, <https://doi.org/10.1016/j.cemconres.2009.09.003>.
- [74] M. R. Jones, M. J. McCarthy, A. McCarthy, Moving fly ash utilisation in concrete forward: A UK perspective, *Proc. Int. ash Util. Symp. Cent. Appl. energy Res. Univ. Kentucky*, no. January, p. #113, 2003.
- [75] S.Y. Choi, I.S. Kim, E.I. Yang, Comparison of drying shrinkage of concrete specimens recycled heavyweight waste glass and steel slag as aggregate, *Materials (Basel)* 13 (22) (2020) 1–15, <https://doi.org/10.3390/ma13225084>.
- [76] K. Gorospe, E. Booya, H. Ghaednia, S. Das, Effect of various glass aggregates on the shrinkage and expansion of cement mortar, *Constr. Build. Mater.* 210 (2019) 301–311, <https://doi.org/10.1016/j.conbuildmat.2019.03.192>.
- [77] R.B. Figueira, R. Sousa, L. Coelho, M. Azenha, J.M. de Almeida, P.A.S. Jorge, C.J. R. Silva, Alkali-silica reaction in concrete: mechanisms, mitigation and test methods, *Constr. Build. Mater.* 222 (2019) 903–931, <https://doi.org/10.1016/j.conbuildmat.2019.07.230>.
- [78] C. Meyer, N. Egosi, C. Andela, *Recycling and reuse of glass cullet*, Thomas Telford Ltd, 2001.
- [79] A. Kashani, T. D. Ngo, A. Hajimohammadi, Effect of recycled glass fines on mechanical and durability properties of concrete foam in comparison with

- traditional cementitious fines, *Cem. Concr. Compos.*, vol. 99, no. October 2017, pp. 120–129, 2019, doi: 10.1016/j.cemconcomp.2019.03.004.
- [80] N. Schwarz, H. Cam, N. Neithalath, Influence of a fine glass powder on the durability characteristics of concrete and its comparison to fly ash, *Cem. Concr. Compos.* 30 (6) (2008) 486–496, <https://doi.org/10.1016/j.cemconcomp.2008.02.001>.
- [81] J. Duchesne, M.A. Béribé, The effectiveness of supplementary cementing materials in suppressing expansion due to ASR: Another look at the reaction mechanisms part 1: concrete expansion and portlandite depletion, *Cem. Concr. Res.* 24 (1) (1994) 73–82, [https://doi.org/10.1016/0008-8846\(94\)90084-1](https://doi.org/10.1016/0008-8846(94)90084-1).
- [82] G.J.Z. Xu, D.F. Watt, P.P. Hudec, Effectiveness of mineral admixtures in reducing ASR expansion, *Cem. Concr. Res.* 25 (6) (1995) 1225–1236, [https://doi.org/10.1016/0008-8846\(95\)00115-S](https://doi.org/10.1016/0008-8846(95)00115-S).
- [83] R. Idir, M. Cyr, A. Tagnit-Hamou, Use of fine glass as ASR inhibitor in glass aggregate mortars, *Constr. Build. Mater.* 24 (7) (2010) 1309–1312, <https://doi.org/10.1016/j.conbuildmat.2009.12.030>.
- [84] G. Lee, T.C. Ling, Y.L. Wong, C.S. Poon, Effects of crushed glass cullet sizes, casting methods and pozzolanic materials on ASR of concrete blocks, *Constr. Build. Mater.* 25 (5) (2011) 2611–2618, <https://doi.org/10.1016/j.conbuildmat.2010.12.008>.
- [85] P.J. Tikalsky, J. Pospisil, W. MacDonald, A method for assessment of the freeze-thaw resistance of preformed foam cellular concrete, *Cem. Concr. Res.* 34 (5) (2004) 889–893, <https://doi.org/10.1016/j.cemconres.2003.11.005>.
- [86] M. Kozłowski, M. Kadelka, Mechanical characterization of lightweight foamed concrete, *Adv. Mater. Sci. Eng.* 2018 (2018) 1–8, <https://doi.org/10.1155/2018/6801258>.
- [87] C. Medina, M.I. Sánchez De Rojas, M. Frías, Freeze-thaw durability of recycled concrete containing ceramic aggregate, *J. Clean. Prod.* 40 (2013) 151–160, <https://doi.org/10.1016/j.jclepro.2012.08.042>.
- [88] X. Tan, W. Chen, H. Tian, J. Yuan, Degradation characteristics of foamed concrete with lightweight aggregate and polypropylene fibre under freeze-thaw cycles, *Mag. Concr. Res.* 65 (12) (2013) 720–730, <https://doi.org/10.1680/macr.12.00145>.
- [89] E. Vasanello, D. Colangiuli, A. Calia, M. Sileo, M.A. Aiello, Ultrasonic pulse velocity for the evaluation of physical and mechanical properties of a highly porous building limestone, *Ultrasonics* 60 (2015) 33–40, <https://doi.org/10.1016/j.ultras.2015.02.010>.
- [90] O.Y. Bayraktar, H. Soylemez, G. Kaplan, A. Benli, O. Gencel, M. Turkoglu, Effect of cement dosage and waste tire rubber on the mechanical, transport and abrasion characteristics of foam concretes subjected to H<sub>2</sub>SO<sub>4</sub> and freeze-thaw, *Constr. Build. Mater.* 302 (2021) 124229, <https://doi.org/10.1016/j.conbuildmat.2021.124229>.
- [91] O. Sengul, S. Azizi, F. Karaosmanoglu, M.A. Tasdemir, Effect of expanded perlite on the mechanical properties and thermal conductivity of lightweight concrete, *Energy Build.* 43 (2–3) (2011) 671–676, <https://doi.org/10.1016/j.enbuild.2010.11.008>.
- [92] W. Pichór, A. Kamiński, P. Szoldra, M. Frąć, Lightweight cement mortars with granulated foam glass and waste perlite addition, *Adv. Civ. Eng.* 2019 (2019) 1–9, <https://doi.org/10.1155/2019/1705490>.
- [93] P. Sikora, E. Horszczaruk, K. Skoczyłas, T. Rucińska, Thermal properties of cement mortars containing waste glass aggregate and nanosilica, *Procedia Eng.* 196 (June) (2017) 159–166, <https://doi.org/10.1016/j.proeng.2017.07.186>.
- [94] J.X. Lu, X. Yan, P. He, C.S. Poon, Sustainable design of pervious concrete using waste glass and recycled concrete aggregate, *J. Clean. Prod.* 234 (2019) 1102–1112, <https://doi.org/10.1016/j.jclepro.2019.06.260>.
- [95] A. Baranova, I. Ryabkov, Investigation of thermal conductivity of non-autoclaved foam concrete based on microsilica, *IOP Conf. Ser. Mater. Sci. Eng.*, vol. 667, no. 1, 2019, doi: 10.1088/1757-899X/667/1/012010.
- [96] F. Koksal, E.T. Kocabeyoglu, O. Gencel, A. Benli, The effects of high temperature and cooling regimes on the mechanical and durability properties of basalt fiber reinforced mortars with silica fume, *Cem. Concr. Compos.* 121 (2021) 104107, <https://doi.org/10.1016/j.cemconcomp.2021.104107>.
- [97] L. Tanacan, H.Y. Ersoy, Ü. Arpacıoğlu, Effect of high temperature and cooling conditions on aerated concrete properties, *Constr. Build. Mater.* 23 (3) (2009) 1240–1248, <https://doi.org/10.1016/j.conbuildmat.2008.08.007>.
- [98] M. Nodehi, S. E. Nodehi, Ultra high performance concrete (UHPC): Reactive powder concrete, slurry infiltrated fiber concrete and superabsorbent polymer concrete, *Innov. Infrastruct. Solut.*, doi: doi.org/10.1007/s41062-021-00641-7.
- [99] P. Mounanga, W. Gbongbon, P. Poullain, P. Turcyn, Proportioning and characterization of lightweight concrete mixtures made with rigid polyurethane foam wastes, *Cem. Concr. Compos.* 30 (9) (2008) 806–814, <https://doi.org/10.1016/j.cemconcomp.2008.06.007>.
- [100] A. Ben Fraj, M. Kismi, P. Mounanga, Valorization of coarse rigid polyurethane foam waste in lightweight aggregate concrete, *Constr. Build. Mater.* 24 (6) (2010) 1069–1077, <https://doi.org/10.1016/j.conbuildmat.2009.11.010>.
- [101] E. Eltayeb, X. Ma, Y. Zhuge, O. Youssf, J.E. Mills, Influence of rubber particles on the properties of foam concrete, *J. Build. Eng.* 30 (December) (2020) 101217, <https://doi.org/10.1016/j.jobe.2020.101217>.
- [102] G.F. Peng, S.H. Bian, Z.Q. Guo, J. Zhao, X.L. Peng, Y.C. Jiang, Effect of thermal shock due to rapid cooling on residual mechanical properties of fiber concrete exposed to high temperatures, *Constr. Build. Mater.* 22 (5) (2008) 948–955, <https://doi.org/10.1016/j.conbuildmat.2006.12.002>.
- [103] T. Gupta, S. Siddique, R.K. Sharma, S. Chaudhary, Effect of elevated temperature and cooling regimes on mechanical and durability properties of concrete containing waste rubber fiber, *Constr. Build. Mater.* 137 (2017) 35–45, <https://doi.org/10.1016/j.conbuildmat.2017.01.065>.
- [104] ASTM C136, Standard Test Method for Sieve Analysis of Fine and Coarse Aggregates - ASTM C136, vol. i, no. 200, pp. 1–5, 2007, doi: 10.1520/C0136-01.